Contribution of Foxp3^{+} regulatory T cells and myeloid-derived suppressor cells to immune homeostasis in the steady state and under inflammatory conditions

Von der Fakultät für Lebenswissenschaften
der Technischen Universität Carolo-Wilhelmina
zu Braunschweig
zur Erlangung des Grades eines
Doktors der Naturwissenschaften
(Dr. rer. nat.)

genehmigte

D i s s e r t a t i o n

von Pedro Milanez de Lima Almeida

aus Moreno, Brasilien

1. Referent Prof. Dr. Michael Steinert

2. Referent Prof. Dr. Jochen Huehn

eingereicht am: 31.03.2014

mündliche Prüfung (Disputation) am: 12.06.2014

Druckjahr 2014

Vorveröffentlichungen der Dissertation

Teilergebnisse aus dieser Arbeit wurden mit Genehmigung der Fakultät für Lebenswissenschaften, vertreten durch den Mentor der Arbeit, in folgenden Beiträgen veröffentlicht:

Publikationen

Milanez-Almeida P., Meyer-Hermann M., Toker A., Khailaie S., Huehn J.: Foxp3^{+} regulatory T cell homeostasis quantitatively differs in murine peripheral lymph nodes and spleen. *In Revision*.

Tagungsbeiträge

Milanez-Almeida, P., Fournier, L., Klages, K., Huehn, J.: Contribution of myeloid-derived suppressor cells to protecting the lung from immunopathology during influenza A infection. (Poster) Annual Retreat of the Helmholtz Graduate School for Infection Research, Hahnenklee (2011).

Milanez-Almeida, P., Fournier, L., Klages, K., Huehn, J.: Contribution of myeloid-derived suppressor cells to protecting the lung from immunopathology during influenza A infection. (Poster) 4th International PhD Symposium of the Helmholtz Graduate School for Infection Research, Braunschweig (2011).

Milanez-Almeida, P., Meyer-Hermann, M., Toker, A., Khailaie, S., Huehn, J.: Consequences of selective depletion of Foxp3^{+} regulatory T cells on the homeostasis of conventional T cells. (Vortrag) Annual Retreat of the Helmholtz Graduate School for Infection Research, Bad Bevensen (2012).

Garg, G., Milanez-Almeida, P., Plaza, C., Ochel, A.: Tolerance: Yin and Yang of T cells. (Vortrag) Annual Retreat of the Helmholtz Graduate School for Infection Research, Hahnenklee (2013).

Milanez-Almeida, P., Meyer-Hermann, M., Toker, A., Khailaie, S., Huehn, J.: Mechanisms of regulatory T cell homeostasis quantitatively differ in lymph nodes and spleen. (Poster) 43. Jahrestagung der Deutschen Gesellschaft für Immunologie, Mainz (2013).

Milanez-Almeida, P., Fournier, L., Klages, K., Huehn, J.: Control of inflammatory responses by infiltrating monocytes under sterile and non-sterile conditions. (Poster) 8th ENII Summer School on Advanced Immunology, Porto Conte, Italien (2013).

Milanez-Almeida, P., Huehn, J.: Selective depletion of Foxp3^{+} regulatory T cells reveals control in a broad immunological context. (Poster) 6th International PhD Symposium of the Helmholtz Graduate School for Infection Research, Braunschweig (2013).

Darüber hinaus wird darauf hingewiesen, dass Abschnitte, Datensätzen und/oder Grafiken dieser Dissertation zum Teil oder vollständig für Veröffentlichungen verwendet werden.

List of Abbreviations

1-MDT	1-Methyl-D-tryptophan
ACK	Ammonium-chloride-potassium
APC	Allophycocyanin
Arg1	Arginase-1
BSA	Bovine serum albumin
CCR	C-C chemokine receptor type
CD	Cluster of differentiation
CFSE	Carboxyfluorescein succinimidyl ester
CO_2	Carbon dioxide
cRPMI	Complemented RPMI
CTLA-4	Cytotoxic T-lymphocyte antigen 4
cTreg	Central Treg
CXCR	Chemokine (C-X-C motif) receptor
Cy	Cyanine
DC	Dendritic cells
DEREG	Depletion of regulatory T cells
DT	Diphtheria toxin
ELISA	Enzyme-linked immunosorbent assay
eTreg	Effector/memory Treg
FACS	Fluorescence-activated cell sorting
FITC	Fluorescein isothiocyanate
Flt3	Fms-like tyrosine kinase 3
Foxp3	Forkhead box P3
HZI	Helmholtz Centre for Infection Research
i.p.	Intraperitoneal
IAV	Influenza A virus
IDO	Indoleamine 2,3-dioxygenase
IFNγ	Interferon-gamma
Ig	Immunoglobulin
IL	Interleukin
iNOS	Inducible nitric oxide synthase
L-NMMA	N^G-Methyl-L-arginine acetate salt

LN	Lymph nodes
Ly6C/G	Lymphocyte antigen 6C/G
MDSC	Myeloid-derived suppressor cells
MHC	Major histocompatibility complex
mo-DC	Monocyte-derived DC
Mono-MDSC	Monocytic MDSC
NK cell	Natural killer cell
NOR-NOHA	N^{ω}-Hydroxy-nor-L-arginine, Diacetate Salt
Nrp1	Neuropilin-1
PBS	Phosphate buffered saline
PE	Phycoerythrin
PerCP	Peridinin chlorophyll protein
PMN-MDSC	Polymorphonuclear MDCS
pTreg	Peripherally induced Treg
RPMI	Roswell Park Memorial Institute Medium 1640
SSC	Side scatter
TGFβ	Transforming growth factor-β
TiP-DC	TNFα/iNOS-producing DC
Tnaïve	Usually naïve $CD4^+$ T cell, used here as synonym for all $CD4^+$ T cells without regulatory function
TNFα	Tumor necrosis factor-α
Treg	Regulatory T cells
tTreg	Thymic Treg

Table of Contents

1. Zusammenfassung

Sowohl unter homöostatischen Bedingungen als auch während einer Entzündung ist die Immunregulation essentiell zum Schutz peripherer Gewebe. In dieser Studie untersuchten wir im stationären Zustand und während einer akuten Infektion die Rolle $Foxp3^+$ regulatorischer T-Zellen (Tregs) und myeloider Suppressorzellen (MDSC), zwei Zellpopulationen mit immunregulatorischen Funktionen. Das erste Ziel war es, verschiedene Mechanismen zu quantifizieren, die zur Treg-Homöostase in wichtigen sekundären lymphatischen Organen beitragen. Dafür wurden *in silico* Modellierung und experimentelle Daten von Treg-Depletion *in vivo* kombinierten und das erste multi-organische mathematische Modell der T-Zell-Homöostase in Mäusen erstellt. Dies wurde in Kooperation mit Prof. Dr. Michael Meyer-Hermann (Abteilung für System-Immunologie, HZI) erreicht. Dieser Ansatz offenbarte Unterschiede in der Homöostase von Tregs und naïven $CD4^+$ T-Zellen (Tnaïves) in peripheren Lymphknoten (LN) und der Milz. So wurde durch das mathematische Model vorhergesagt, dass Treg-Induktion für die Aufrechterhaltung der Treg-Population in LN relevanter ist als in der Milz. Die Ergebnisse führten zu der Schlussfolgerung, dass sich die Mechanismen der Treg-Homöostase in LN und der Milz quantitativ unterscheiden. Das zweite Ziel war es zu untersuchen, ob andere Immunzellpopulationen von der Treg-Depletion *in vivo* betroffen sind. Dies könnte unser Wissen darüber erweitern, wie Tregs das immunologische Gleichgewicht im stationären Zustand kontrollieren. Wir haben beobachtet, dass sich eine Reihe von Immunzellpopulationen wie dendritische Zellen, natürliche Killerzellen und myeloide Zellen in LN und der Milz in Abwesenheit von Tregs anhäuft. Interessanterweise unterschieden sich die Kinetik dieser Akkumulation in LN und der Milz, was darauf hinweist, dass Immunregulation in diesen Organen möglicherweise unterschiedlich erreicht wird. Schließlich haben wir die Rolle von MDSC während einer akuten Infektion mit dem Influenza-A-Virus (IAV) untersucht. Da es bekannt ist, dass IAV eine starke Immunantwort mit folgenden Lungenschäden auslösen kann, könnte dies neue Wege enthüllen, die einen Beitrag zur Immunregulation in infizierten Lungen leisten. Die Daten der vorliegenden Arbeit zeigten, dass IAV eine

Akkumulation von monozytären-MDSC (mono-MDSC) in infizierten Mäusen induziert. IAV-induzierte mono-MDSC wiesen die Fähigkeit auf, *in vitro* die Proliferation von T-Zellen zu unterdrücken. Der Mechanismus der Unterdrückung war abhängig von iNOS, dessen Expression *in vivo* von IFNγ abhing. Bisher wurde davon ausgegangen, dass Monozyten und iNOS eine pro- aber nicht eine anti-inflammatorische Rolle nach IAV-Exposition spielen. Die Ergebnisse der vorliegenden Arbeit führen somit zu einer Neubewertung der Rolle von Monozyten und iNOS während einer IAV-Infektion. Insgesamt hilft diese Studie dabei, unser Verständnis zu erweitern, wie Immunregulation durch Tregs und MDSC im stationären Zustand und während einer Entzündung aufrechterhalten wird.

2. Abstract

Immune regulation is essential to protect peripheral tissues under homeostatic conditions as well as during inflammation. In this study, the role of forkhead box P3 (Foxp3)-expressing regulatory T cells (Tregs) and myeloid-derived suppressor cells (MDSC), two cell populations with immune regulatory functions, was investigated in the steady state and in acute infection, respectively. The first aim was to quantify different mechanisms contributing to Treg homeostasis in major secondary lymphoid organs. Thereto, *in silico* modeling and experimental data from *in vivo* Treg depletions were combined to build the first multi-organ mathematical model of T cell homeostasis in mice, which was accomplished in co-operation with Prof. Dr. Michael Meyer-Hermann (Department of Systems Immunology, HZI). This approach revealed, for example, differences in the homeostasis of Tregs and naïve $CD4^+$ T cells (Tnaïves) as well as in their response to Treg depletion when comparing their populations in peripheral lymph nodes (LN) and spleen. Furthermore, the mathematical model predicted Treg induction to be more relevant for maintenance of the Treg population in LN than in the spleen. These results led to the conclusion that the mechanisms contributing to Treg and Tnaïve homeostasis in LN and spleen quantitatively differ. The second aim was to examine whether immune cell subsets other than Tnaïves are affected by Treg depletion *in vivo*. This could expand the knowledge on how Tregs maintain immune homeostasis in the steady state. It was observed that a range of immune populations, such as dendritic cells (DC), natural killer (NK) cells and myeloid cells, accumulate in LN and spleen in the absence of Tregs. Interestingly, the kinetics of this accumulation differed in LN and spleen, pointing out that immune regulation might be differently achieved in these organs. The last aim was to examine the role played by MDSC during acute infection with influenza A virus (IAV). Since IAV is known to induce an overwhelming immune response associated with lung damage, this could unveil new pathways contributing to immune regulation in infected lungs. The data demonstrate that IAV induces accumulation of monocytic MDSC (mono-MDSC) in infected mice. IAV-induced mono-MDSC had the ability to suppress T cell proliferation *in vitro*. The mechanism of suppression applied by mono-

MDSC was dependent on iNOS expression, the expression of which depended on IFNγ *in vivo*. So far, monocytes and iNOS were believed to play a pro- but not an anti-inflammatory role upon IAV challenge. Thus, the results of the present study might lead to a reconsideration of the role of monocytes and iNOS in IAV infection. Altogether, this study helps to expand the understanding of how immune regulation is maintained by Tregs and MDSC in the steady state and during inflammation.

3. Introduction

Understanding immune regulation might help intervening in a number of diseases, including autoimmunity, cancer, allograft rejection, allergy and infection. For example, the importance of immune regulation during infection can be observed in the immune response to sepsis and flu, when the immune system might overreact and damage own tissues, leading to pathology and death. Other examples come from invasion by pathogens able to induce immune tolerance, such as observed in viral hepatitis or different parasitic infestations. Here, low-levels of effector immune responses allow pathogen persistence, which is associated with latent disease and health burden. Additionally, studying immune regulation might help the in development of strategies to boost vaccination, aiming at improving protection against infections at the population levels. Therefore, understanding regulatory immune cells, which play are central role in the control of immune responses, might open new avenues for the prevention and treatment of a number of pathologies. Two subsets of regulatory immune cells able to induce tolerance are in the focus of the present study: Tregs and MDSC. Although both are known for decades now, many questions regarding their biology have still to be addressed, as introduced below.

3.1. Tregs

The vast majority of immune reactions are orchestrated by different $CD4^+$ T cell subsets. Among these subsets, Tregs are specialized in immunosuppression and are essential for maintenance of immune homeostasis and prevention of autoimmunity [1]. Due to promising therapeutic applications, such as avoiding autoimmune diseases, promoting tolerance towards allografts and as target in cancer immunotherapies [2; 3], enormous efforts have been made to comprehensively investigate Treg development, homeostasis and function.

3.1.1. Importance of the transcription factor Foxp3

Treg function is controlled by the transcription factor Foxp3 [4-6], which was first described in 2001 when the association between mutated *foxp3* gene

and both murine fatal lymphoproliferative disorder and human immune dysregulation, polyendocrinopathy, enteropathy, X-linked syndrome was discovered [7-9]. Foxp3 expression is of key importance for the immunosuppressive phenotype of Tregs [10; 11], and it has been demonstrated that epigenetic control of *foxp3* and other Treg-associated genes leads to the stabilization of the Treg phenotype and to the fixation of the Treg lineage [12-15]. Among these genes are, for example, c*tla4* (encoding for cytotoxic T-lymphocyte antigen 4) and *il2ra* (encoding for the high affinity IL-2 receptor α chain, also known as CD25). Indeed, CTLA-4 and CD25 play central roles in Treg function. CTLA-4 binds to CD80 and CD86, co-stimulatory molecules on the surface of DC, dampening DC interaction with effector T cells [16; 17]. CD25 form the high affinity IL-2 receptor in combination with CD122 (low affinity IL-2 receptor β chain) and CD132 (common γ chain). It efficiently binds and consumes IL-2, a survival and growth factor for effector T cells [18]. In addition to mediating suppressive activity by Tregs, CD25, as part of the IL-2 receptor complex, is central for the enhanced IL-2 sensitivity and signaling in Tregs, which is essential for Treg homeostasis in the periphery [19; 20]. Foxp3 binds to the IL-2 promoter and blocks IL-2 expression in Tregs [21], making them dependent on IL-2 produced by Tnaïves and creating a Tnaïve/IL-2/Treg feedback control mechanism. Therefore, Foxp3 controls Treg function by controlling the expression of molecules involved in Treg homeostasis as well as by fine-tuning the expression of molecules directly involved in Treg-mediated suppression.

3.1.2. Thymic and peripheral development of Tregs

T cell selection takes place in the thymus, where T cell progenitors carrying a newly generated T cell receptor with high affinity for self-antigens are deleted. This view has been challenged by the observation that recognition of self-antigens in the thymus can also induce Foxp3 expression in progenitor T cells leading to the development of thymic Tregs (tTregs) [22]. Furthermore, Tnaïves circulating in the periphery can, under certain conditions, upregulate Foxp3 expression and give rise to peripherally induced Tregs (pTregs). While

tTregs are believed to mainly recognize self-antigens, pTregs might complement the Treg repertoire by specificities directed against non-pathogenic foreign antigens, including commensal microbiota and food antigens [22-26]. Due to the difference in the nature of antigens recognized by tTregs (self) and pTregs (non-self), it is generally considered that these populations have different niches and, thereby, different functions [27], although this might not be the case under certain conditions [28]. In this regard, further studies are necessary before drawing definitive conclusions. Estimating the distribution of tTregs versus pTregs within the peripheral Treg pool is still a matter to be resolved. Recently, Helios and Neuropilin-1 (Nrp1) have been reported as markers to distinguish tTregs and pTregs *in vivo* in the steady state [28-31]. However, both markers can also be upregulated in pTregs in the course of T cell activation and differentiation [31; 32]. Further investigations on the role of tTregs and pTregs in immune homeostasis are necessary, since this could improve the knowledge on immune regulation towards self and non-self.

3.1.3. Diversity and specialized functions of Treg subsets

Tregs are involved in suppressing both initiation as well as the effector phase of an immune response [33]. Accordingly, Tregs were sub-divided into central Tregs (cTregs), which recirculate and inhibit T cell priming in secondary lymphoid organs, and effector/memory Tregs (eTregs), able to migrate to peripheral tissues and inhibit inflammation *in situ*. Differential expression of adhesion molecules and chemokine receptors provides cTregs and eTregs, commonly characterized as $CD62L^{+}CD44^{-}CCR7^{+}$ and $CD62L^{-}CD44^{+}CCR7^{-}CD103^{+}$, respectively, proper anatomical localization and corresponding suppressive activity [34]. Figure 1 summarizes how Treg homeostasis is maintained. In the steady state, tissue-resident eTregs are essential for homeostasis of the gut and adipose tissues, for example, which is mechanistically achieved, among others, by IL-10 production [35; 36]. Upon inflammation, eTregs expand and accumulate, for example, in the skin and skeletal muscles, where they play a distinct role in the resolution of the immune response [37; 38]. It was discussed that this is accomplished by a

CTLA-4-dependent mechanism and by promotion of a switch from pro-inflammatory to anti-inflammatory myeloid cells, respectively [37; 38]. Interestingly, eTregs in skeletal muscle express amphiregulin upon injury and can thereby directly promote muscle repair by acting on muscle satellite cells [38]. In addition, it is currently a matter of discussion whether the transcriptional control of eTregs matches those of T helper subsets. Th1, Th2, Th17 and follicular T helper (Tfh) cells are specialized effector T cell subsets expressing distinct transcription factors – T-bet, GATA3, RORγt/STAT3 and BCL-6, respectively – and orchestrating distinct immune responses. Expression of Th-associated transcription factors by Tregs could lead to optimal ability to suppress specific Th responses [39]. Lack of T-bet or BCL-6 in Tregs, for example, prevent expression of the chemokine receptors CXCR3 and CXCR5, respectively, making Tregs unable to relocate to the corresponding anatomical sites where Th1 and Tfh cells are present and exerting their functions [40; 41]. Upon arrival at these sites, eTregs expressing Th-specific transcription factors upregulate expression of suppressor molecules such as IL-10, transforming growth factor-β (TGFβ) and granzyme B [40; 41]. The Treg diversity reflects the importance of this immune cell subset for maintenance of immune balance in different settings. It seems therefore quite surprising that quantitative data on the mechanisms leading to a stable Treg population in the periphery, such as thymic output, peripheral conversion, activation, proliferation, migration and apoptosis is still missing.

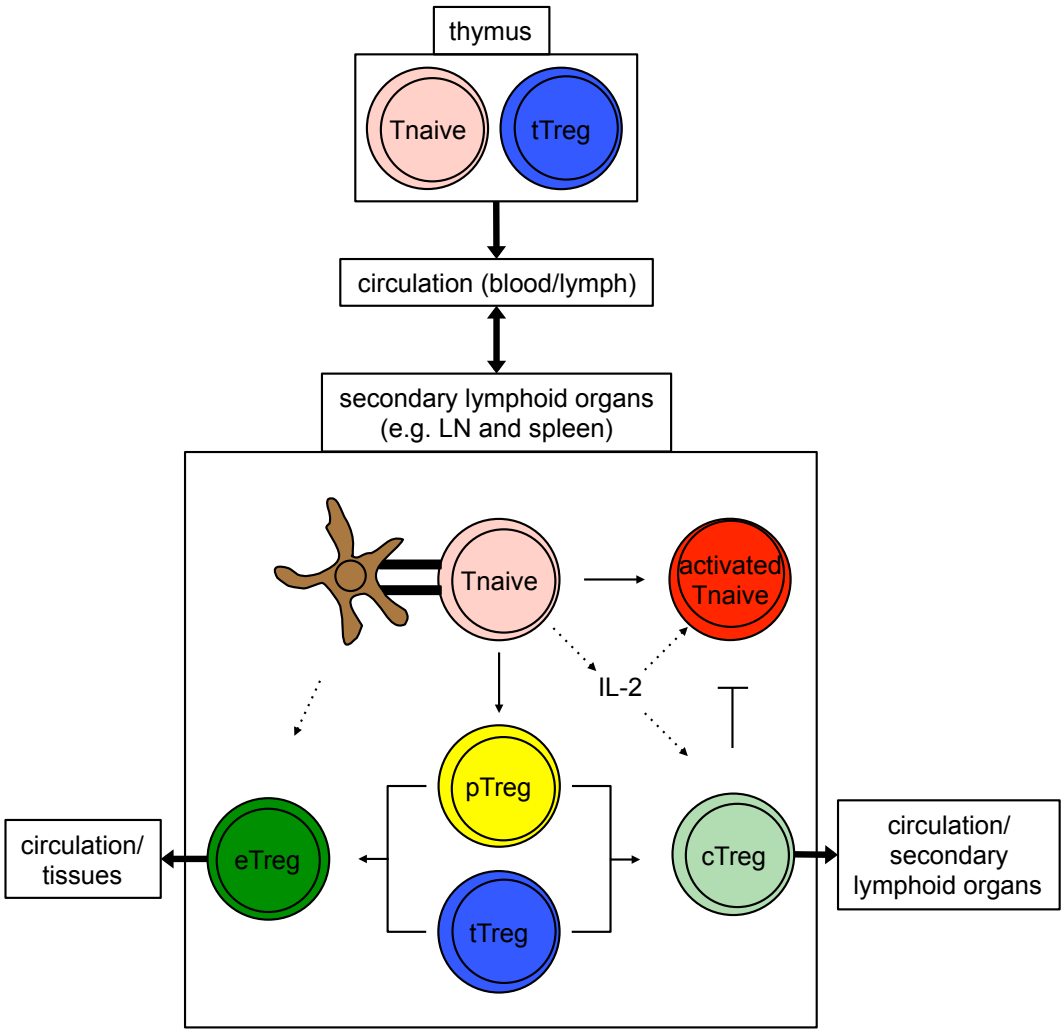

Figure 1: Treg homeostasis in secondary lymphoid organs.
Tnaïves and tTregs leave the thymus via the circulation and reach secondary lymphoid organs. Tnaïves might encounter DC and either become activated, producing IL-2, or be converted into pTregs. Both pTregs and tTregs might become eTregs or cTregs, the survival of which depends on DC interaction and Tnaïve-derived IL-2, respectively [34]. Tregs can avoid Tnaïve activation by consuming IL-2 and suppressing DC/Tnaïve interactions (not depicted). cTregs reenter circulation and survey secondary lymphoid organs, while eTregs reenter circulation and survey peripheral tissues.

3.1.4. Interaction of Tregs with other immune cell subsets

Besides their role in controlling effector T cells, Tregs were described to directly and indirectly regulate other immune cell subsets. DC are considered the hub of the immune system. This innate cell type senses signals in the environment they are located and migrate towards secondary lymphoid organs to initiate and shape the adequate adaptive immune response [42;

43]. In the steady state, the size of the DC population seems to be tightly controlled by the size of the Treg population [44; 45]. A loss in Tregs leads to a gain in DC, which in turn induces an expansion of Tregs. This feedback loop is controlled by Flt3 [44; 45]. NK cells are innate lymphocytes which become activated, among others, by IL-2 and are able to limit virus and tumor growth before adaptive immunity is mounted [46]. The homeostasis of the NK cell population is also modulated by Tregs. Treg-mediated IL-2 consumption and inhibition of IL-2 production in Tnaïves play a central role in NK cell homeostasis [47-49]. Furthermore, under inflammatory conditions, Tregs can suppress effective B cell responses, suppressing antibody production [50-52]. Interestingly, although no B cell intrinsic role for Foxp3 was found, B cell development is defective in Foxp3-deficient mice [52; 53]. However, since these animals suffer from severe multi-organ autoimmune disease, it is difficult to distinguish between effects on B cells caused directly by Treg absence from those caused by systemic inflammation. Keeping in mind that Treg depletion in clinical setting has been proposed as strategy to improve immunotherapy and vaccination, it is of central relevance to conclusively establish whether and how Tregs regulate homeostasis of other immune cell subsets.

3.2. MDSC

As discussed above, Tregs are a constitutive part of the immune system, appearing in circulation just some days after birth and controlling the immune system throughout life. Differently, MDSC can only be observed under inflammatory conditions and were described to appear in cancer, chronic inflammation, physical trauma and some infections [54; 55]. Therefore, the development of MDSC is currently considered pathological and their presence is associated with an ineffective immune response. Much effort has been put into characterizing the origin and mechanisms of function of MDSC, as they represent potential targets for immunotherapies in the clinics [56].

3.2.1. Development of monocytes, granulocytes and their progenitors into MDSC

It has become increasingly clear that mono-MDSC arise from $CD11b^{+}Ly6C^{++}Ly6G^{-}$ monocytes and monocyte progenitors, which is an innate cell lineage developing in the bone marrow and responding to stimuli with an impressive plasticity. In the absence of inflammation, $Ly6C^{++}$ monocytes give rise to Nr4a1-dependent $Ly6C^{-}$ monocytes, which are readily found within capillaries, surveying endothelial cells and coordinating their disposal [57; 58]. For means of simplification and because $Ly6C^{-}$ monocytes are far less well described than their $Ly6C^{++}$ counterpart, the term monocytes will be used in this study to refer only to $Ly6C^{++}$ monocytes. At low levels of inflammation, such as in atherosclerosis, some types of cancer and in the healthy gut, monocytes can differentiate into tissue-associated macrophages, upregulating markers corresponding to the macrophage lineage and participating in tissue homeostasis [59-61]. In acute inflammation, such as in acute bacterial and viral infections, they can differentiate into professional antigen-presenting cells and migrate to the draining LN [62]. At this stage they are commonly called “monocyte-derived” (mo-) DC, with the ability to initiate a T cell response. Acute inflammation can lead monocytes also to fight infection *in situ* via production of cytokines and effector molecules, such as tumor necrosis factor-α (TNFα) and inducible nitric oxide synthase (iNOS), a state in which they are called “TNFα/iNOS-producing” (TiP-) DC [63-65]. Both mo-DC and TiP-DC have upregulated expression of DC markers. In chronic inflammation, such as chronic infection or in cancer, monocytes can acquire suppressive activity towards T cells, a state in which they are known as mono-MDSC [66]. Interestingly, no markers were found so far with expression restricted to mono-MDSC but missing in other monocyte-derived subsets. Indeed, until recently, studying MDSC biology by flow cytometry was confused as the anti-Gr1 antibody, actually recognizing granulocytes but widely used for MDSC studies in the past, binds to two different molecules, Ly6C and Ly6G. The use of antibodies able to distinguish Ly6C and Ly6G led the way to the description of at least two subsets of MDSC: mono-MDSC ($CD11b^{+}Ly6C^{++}Ly6G^{-}$) and polymorphonuclear MDSC (PMN-MDSC,

$CD11b^{+}Ly6C^{+}Ly6G^{+}$) [66-69].

The general assumption that mono-MDSC derive from subverted monocytes and their progenitors is mainly due to their similar morphology and expression of surface markers. Further indication came from studies of CCR2, a chemokine receptor responsible for bone marrow exit of monocytes and, thereby, for their accumulation at sites of inflammation [70]. CCR2 deficiency leads to a reduction in the accumulation of monocytes and TiP-DC at infection sites [63; 64] as well as to a reduction in the number of monocytes and MDSC at tumor sites [67; 69]. Also due to similarities in morphology and surface markers, PMN-MDSC are thought to arise from subverted granulocytes and granulocyte progenitors [55]. However, a recent report described that mono-MDSC differentiate into PMN-MDSC in tumor-bearing mice as well as in cancer patients [71]. According to that model, mono-MDSC acquire Ly6G expression as well as granulocyte-like morphology and function, in a process regulated by the retinoblastoma gene [71]. Altogether, the similarities of monocytes, granulocytes and their progenitors with mono-MDSC and PMN-MDSC with regard to their morphology, surface markers and response towards chemokines as well as the differentiation of mono-MDSC into PMN-MDSC indicate a complex MDSC developmental pathway. Briefly, MDSC development is considered to start under chronic inflammatory conditions with monocytes and progenitors giving rise to mono-MDSC, which, together with granulocytes and progenitors, further differentiate into PMN-MDSC (Fig. 2).

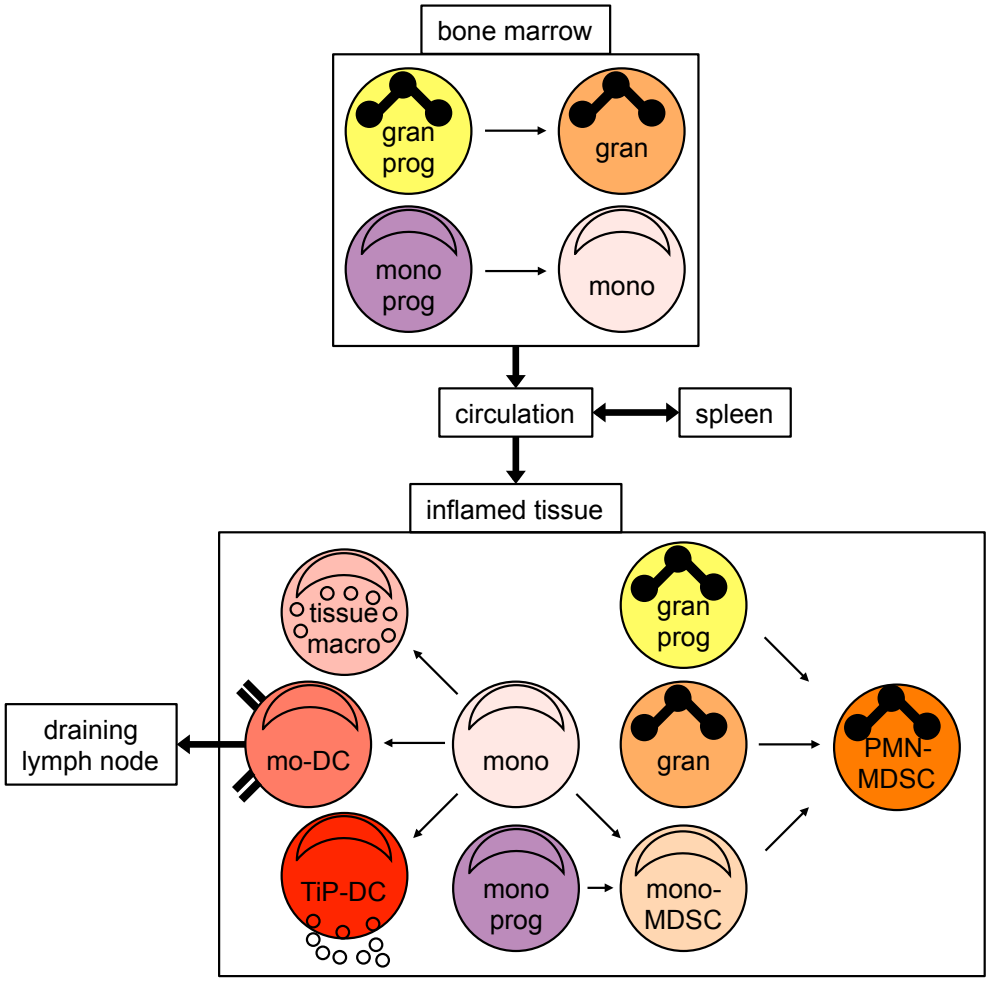

Figure 2: Monocytes and granulocytes during inflammation.
Granulocyte progenitors (gran prog) and monocyte progenitors (mono prog) differentiate into granulocytes (gran) and monocytes (mono) in the bone marrow. During inflammation, they travel via the circulation, passing the spleen, while seeking for the inflamed tissue. Upon arrival at inflamed tissues, monocytes can further differentiate into tissue-associated macrophages (tissue macro), mo-DC and TiP-DC according to microenvironmental clues (see main text). Alternatively, monocytes and their progenitors can become mono-MDSC. Granulocytes, granulocyte progenitors and mono-MDSC can give rise to PMN-MDSC. MDSC can also develop and accumulate in the spleen (not depicted).

3.2.2. MDSC-mediated suppression and their role in infection

Among the most studied mechanisms that MDSC apply to modulate an immune response is the inhibition of T cells [54]. MDSC can induce nitration of tyrosines at the T cell receptor, disrupting antigen recognition and T cell activation, they can induce Tregs, which are suppressive by themselves, and they can produce anti-inflammatory cytokines such as IL-10 and TGFβ [72-

76]. Another mechanism of MDSC-mediated T cell suppression involves consumption of the semi-essential amino acid arginine by the enzymes iNOS and arginase-1 (Arg1), leading to production of reactive nitrogen and oxygen species such as nitric oxide (NO), peroxynitrites, superoxide, and hydrogen peroxide, which are themselves cytotoxic and inhibitory [54]. Expression of indoleamine 2,3-dioxygenase (IDO), which degrades the amino acid tryptophan, can also be used by MDSC to perform immunosuppressive activity [77; 78]. So far it is not completely understood why some mechanism of suppression predominates over others in different inflammatory settings.

Although MDSC are best known for their role in immune suppression in cancer, there are several reports on the development of MDSC during infection. In polymicrobial sepsis, for example, MDSC play a protective role by dampening excessive inflammation and preventing tissue damage [79]. In candidiasis, MDSC are detrimental as they disrupt an effective Th1-mediated anti-fungal response [80]. MDSC were also shown to develop during chronic infections with human immunodeficiency virus type 1 and lymphocytic choriomeningitis virus [81; 82]. However, evidence for MDSC accumulation during acute viral infection was only reported for vaccinia virus [83], so that their role in other acute viral infections still has to be addressed.

3.2.3. IAV infection

Immune regulation is especially important in the context of an acute infection of the respiratory tract with IAV, since lethality here is caused by inflammation-induced lung destruction [84; 85]. Usually, IAV infection triggers mild symptoms such as fever, cough and sore throat. However, the number of deaths in a year can substantially incresase if the virus strain circulating in that season shows high pathogenicity [86]. For instance, the number of deaths in Germany increased by a 60-fold factor, from 300 to 18000, when comparing the 2007/08 and the 2008/09 seasons [86]. In addition, the disease can become pandemic, which was observed in 1918 with the Spanish flu and in 2009 with the swine flu [87; 88]. Challenges with vaccination, which respresents the gold standard for protection against IAV, come from antigenic drifts and shifts as well as from problems in vaccine

production itself [89]. Therefore, it is essential to better comprehend this multifaceted, life-threatening and highly pandemic disease.

IAV belongs to the family of *Orthomyxoviridae* viruses and, although having wild aquatic birds as natural reservoirs, can infect domestic poultry and mammals [90]. Its genetic material is encoded in eight segments of negative-sense RNA, which contain the information for the expression of its eleven proteins [91]. Among these proteins, haemagglutinin (HA) and neuraminidase (NA), two IAV surface proteins, are categorized into different subtypes, which is commonly used for classification of virus strains [90; 91]. For example, if a strain carries HA subtype 1 and NA subtype 1, it is classified as H1N1. The H7N9 strain spreading in Asia to date and causing human infection and death upon exposure to contaminated poultry carries HA subtype 7 and NA subtype 9 [92]. HA has two functions; on one hand, it recognizes sialic acid on the surface of target cells and, on the other, it promotes entry of the virus genome into the cell by facilitating fusion of the virus membrane with the endosomal membrane [93]. NA enzymatically cleaves sialic acid on the surface of infected cells, allowing IAV to be released and to infect new cells [94]. Antibodies that bind to HA and NA and block their functions are important for protection against new infections. However, HA and NA mutate rapidly in the host cell, changing the ability of pre-formed antibodies to bind to them. This phenomenon of gradual changes in HA and NA leads to escape from acquired immunity and is called antigenic drift [95]. It is also the reason why, for optimal protection against emerging infections, the strains used for vaccination have to be updated every season [89]. Besides the constant mutations causing continuous IAV antigenic drift, the virus can also evolve through abrupt, wide-ranging but rare steps known as antigenic shifts [95]. In case one cell is infected by two different IAV strains, the genetic material of both strains can randomly recombine and a completely new virus can be originated. Such reassortment events are believed to have generated the novel H7N9 Asian strain [96].

Although some IAV strains can infect different species, usually species-specificity is observed. Important for species-specificity is, among others, the

ability of HA to bind to receptors on host cells [97; 98]. HA from different IAV strains bind to sialic acid residues with different linkages. For example, HA from strains of human origin usually binds to sialic acid residues with a 2-6 linkage (SA α-2,6) whereas HA from strains of avian origin bind to sialic acid residues with a 2-3 linkage (SA α-2,3) [97; 98]. This seems to be an adaptation to the differential tissue distribution of sialic acid residues is different species. While humans predominantly have SA α-2,6 moieties in the respiratory tract, avian species have SA α-2,3 moieties in the gastrointestinal tract [97; 98]. Interestingly, mice possess SA α-2,3 moieties in their respiratory tract but lack SA α-2,6 moieties, which might explain why human IAV strains usually have to be adapted prior to successfully infecting mice [99]. Since ferrets resemble humans with regard to tissue distribution of SA α-2,6 moieties, leading to disease development being highly similar to the human infection, they are often used as animal model for IAV studies [100]. Despite such disadvantages, use of the murine model of IAV infection vastly contributed to understanding of IAV-induced pathology as well as of IAV-evoked immune response [97; 98].

3.2.4. Immune response to IAV and the detrimental role of monocytes and their progeny

Adaptive immunity is essential for the host to fight disease. Plasma cells generated during first exposure efficiently produce antibodies that block HA and NA from related strains to neutralize the virus [101]. Response by memory T cells is also important, as revealed in so-called heterosubtypic immunity experiments [102]. Hereto, mice that recovered from a first infection are exposed to another strain carrying different HA and NA subtypes (i.e. antibodies from the first infection cannot block the second one). Such experiments demonstrated that T helper cells and cytotoxic $CD8^+$ T cells (CTL) predominantly respond to epitopes from conserved proteins and mediate protection of heterosubtypically infected mice [102]. During primary infection, both CTL and T helper cells play a determinant role. CTL are essential for virus clearance via lysing infected cells in a contact-dependent manner, while T helper cells support B cell production of antibodies [103].

Remarkably, T helper cells were also shown to help CTL production of IL-10 during primary IAV infection, which was fundamental for mice to keep immune balance and avoid lung immunopathology while efficiently clearing the virus [104]. Tregs are also involved in the immune response against IAV. During primary infection virus antigen-specific Tregs robustly expand in the infected lungs whereas during secondary infection they avoid CTL-mediated lung inflammation [105; 106]. Therefore, the host developed different strategies to fight IAV infection while assuring immune balance in the delicate lung tissues.

Notably, lethal IAV infection in mice is tremendously attenuated if the number of monocytes and TiP-DC in the lungs is experimentally reduced [65; 107]. Based on these studies, monocytes and TiP-DC were interpreted as major inducers of lung inflammation during IAV infection [108]. In this context, the differentiation of lung infiltrating monocytes into MDSC was not considered, although some initial studies showed that MDSC might be involved. For example, monocytes with anti-inflammatory activity were shown to improve the outcome of IAV infection when pre-activated *in vivo* by *Staphylococcus aureus* products [109]. On the other hand, mice deficient of invariant NK T cells and infected with IAV display an overgrowth of MDSC, which impaired a proper T cell response to the virus [110]. Therefore, the role of monocyte differentiation into mono-MDSC during IAV infection is not clear and should be addressed to provide a better understanding of immune regulation in this infection.

4. Aims

This thesis consists mainly of two parts. The first focused on Tregs and their role in keeping immune homeostasis, whereas the second concentrated on the role of MDSC during IAV infection.

Although Treg homeostasis is of vital importance for mice and men [7-9; 111; 112], quantitative data on the different processes maintaining Treg stability at the population level are only scarcely available. The first part of this study aimed at a more refined understanding of Treg homeostasis. Thereto a combined *in vivo* and *in silico* approach was used to quantify the contribution of thymic output, peripheral conversion, migration, proliferation and apoptosis of Tregs and Tnaïves to Treg homeostasis in major secondary lymphoid organs.

The role of Tregs in keeping immune homeostasis by modulating the function of T cells, DC and NK cells is well established [18; 44; 45; 113]. Less clear is the influence of Tregs on other immune cells such as B cells and myeloid cells. The next aim here was to analyze the kinetics of different immune populations in the absence of Tregs in different secondary lymphoid organs. Thereto, the depletion of regulatory T cells (DEREG) mouse model was used, which allows for selective ablation of $Foxp3^+$ Tregs *in vivo* without development of severe multi-organ autoimmune disease. Since Treg depletion in clinical settings is a major goal of on going translational research, it is highly appropriate to examine how Tregs influence homeostasis of other cell subsets of the immune system.

MDSC hamper a proper immune response in cancer and different infections [54; 55]. Less well studied is their role during acute viral infection. The second part of this work aimed at investigating whether MDSC play a role during IAV infection, which is known for the role of monocytes in inducing lung damage and enhanced pathology. The murine IAV infection model was used to characterize the phenotype of lung mono-MDSC as well as their function and kinetics. The mechanistic role of different amino acid cleaving enzymes in mono-MDSC-mediated suppression was also examined. Since immune regulation by MDSC might have a protective role during acute infections

characterized by inflammation-induced tissue destruction, it might be of great relevance to study MDSC in the context of IAV infection.

5. Material and Methods

5.1. Material

5.1.1. Buffers and Solutions

PBS/BSA	Phosphate-buffered saline (PBS, Invitrogen, Karlsruhe) 0.2 % BSA (Sigma-Aldrich, Deisenhofen)
ACK buffer	Sterile Milli-Q water 0.01 M $KHCO_3$ (Sigma-Aldrich) 0.155 M NH_4Cl (Sigma-Aldrich) 0.1 mM Ethylenediaminetetraacetic acid (Roth, Karlsruhe) pH 7.5
cRPMI	Roswell Park Memorial Institute (RPMI) Medium 1640 - GlutaMAX™ (Invitrogen) 10 % fetal calf serum (FCS; Sigma-Aldrich) 50 U/ml Penicillin (Biochrom, Berlin) 50 U/ml Streptomycin (Biochrom) 25 mM HEPES (Biochrom) 1 mM Sodium Pyruvate (Biochrom) 50 µM β-mercaptoethanol (Biochrom)
Digestion buffer	Iscove's Modified Dulbecco's Medium (IMDM; Invitrogen) 10 % fetal calf serum (FCS; Sigma-Aldrich) 0.2 mg/ml collagenase D (Roche, Mannheim) 10 mg/ml DNAse (Roche) 0.8 U/ml Dispase (Roche), added after 30 min of digestion

5.1.2. Antibodies

The amount of antibodies needed for each staining was previously defined by titration series.

Table 1: Antibodies used for flow cytometry. All antibodies were from eBioscience (San Diego, CA, USA), BioLegend (San Diego, CA, USA), BD Biosciences (Franklin Lakes, NJ, USA), Santa Cruz Biotechnology (Santa Cruz, CA, USA) or R&D Systems (Minneapolis, MN, USA).

Specificity	Fluorochrome	Clone
CD3	Biotin, eFluor450, FITC, PE-Cy7, APC	17A2, 145-2C11
CD4	Pacific Blue, PerCP-Cy5.5, PE-Cy7, APC, Alexa Fluor 750	RM4-5
CD8	Horizon V500	53-6.7
CD11b	eFluor450, FITC, PE-Cy7, APC-Cy7	M1/70
CD11c	FITC, PerCP-Cy5.5, PE, APC, APC-eFluor780	N418
CD19	Biotin, APC	MB19-1
CD25	PE-Cy7	PC61.5
CD44	PerCP-Cy5.5, APC	IM7
CD45R	Pacific Blue, PerCP-Cy5.5, PE-Cy7, APC, APC-eFluor780	RA3-6B2
CD49b	Biotin, FITC, PE-Cy7, APC	DX5
CD62L	FITC	MEL-14
CD69	PE-Cy7	H1.2F3
CD86	PE	GL1
CD90.2	PE	53-2.1
CD122	Biotin	TM-b1
CD335	PerCP-Cy5.5, APC	29A1.4
Foxp3	Alexa Fluor 488, PE, Alexa Fluor 647	FJK-16s
iNOS	Alexa Fluor 647	C-11
Ly6C	eFluor450, Alexa Fluor 488, APC	HK1.4
Ly6G	PE-Cy7	1A8
MHCII	FITC, Alexa Fluor 700	M5/114.15.2
Nrp1	Biotin	polyclonal
Streptavidin	PE, PE-Cy7, APC-Cy7	-

5.2. Methods

5.2.1. Mice

DEREG mice and wildtype littermates (BALB/c background) were bred at the animal facility of the HZI. Eight to twelve weeks old male mice were used. C57BL/6 mice for the IAV murine infection model were either bred at the animal facility of the HZI or purchased from Janvier (Le Genest-Saint-Isle, France). Ten to fourteen weeks old female mice were used here. All animal experiments were performed under specific pathogen-free conditions and in accordance with institutional, state and federal guidelines.

5.2.2. DT and Treg depletion

For Treg depletion *in vivo*, DEREG mice and wildtype littermates were injected by intraperitoneal (i.p.) with 1 µg DT (Merck/Calbiochem, Darmstadt; stored at -70 °C until use) diluted in 100 µl sterile PBS (Gibco). DEREG mice and wildtype littermates treated with PBS were used as controls (d0). Mice were sacrificed at indicated time points and cells from LN and spleen were isolated and analyzed.

5.2.3. Virus preparation and mouse infection

Mouse-adapted influenza A/Puerto Rico/8/34 (H1N1 PR8) virus strain was kindly provided by Prof. Dr. Klaus Schughart and Christin Fricke (Department of Infection Genetics, HZI). Intranasal infection was performed with one tenth of the median lethal dose (LD_{50}) as defined before for the used virus batch (2 x 10^4 focus forming viral units/mouse in 20 µl PBS) [114]. Thereto, mice were anesthetized prior to infection by i.p. injection of ketamine, a dissociative anesthetic, and xylazine, a sedative/analgesic (10 mg/ml ketamine and 1 mg/ml xylazine diluted in PBS; 10 µl/g of body weight). Ophthalmic ointment was applied to prevent drying of the corneas and mice were kept insulated to avoid loss of body heat. Healthy status and body weight were checked every second day. Mice losing more than 20 % of body weight within two days were euthanized and the infection considered lethal. I.p. injection of 1 mg of either anti-IFNγ (R4-6A2) or rat IgG isotype control (HRPN) antibodies from

BioXCell (West Lebanon, NH, USA) was performed on day 5 after infection. Mice were sacrificed at indicated time points and cells from spleen and lung were isolated and analyzed.

5.2.4. Organ isolation and preparation of single cell suspensions

Mice were sacrificed by CO_2 asphyxia and spleen, LN and/or PBS-perfused lungs were taken. Lungs were minced and digested at 37 °C for a total of 45 min in digestion buffer (see “Buffers and Solutions”). Lung digestion was stopped by adding EDTA (ethylenediaminetetraacetic acid) to a final concentration of 5 mM and by keeping samples on ice. Single cell suspensions were prepared by mechanical squeezing of LN, minced spleens or digested lungs through 100 µm nylon meshes. Erythrocytes in spleen and lung samples were lysed by incubation with ammonium-chloride-potassium (ACK) buffer for 4 minutes at room temperature. Lysis was stopped by diluting ACK buffer in a 10-fold volume of PBS/BSA. Centrifugation steps were at 4 °C and 450 g for 8 minutes. If not described otherwise, samples were subsequently maintained in PBS/BSA.

5.2.5. Cell staining

Dead cells were stained using LIVE/DEAD® fixable dead cell stain kit (Invitrogen), as by the manufacturer. Specific antibody staining was performed at 4 °C in the dark for 15 min (surface staining) or 30 min (intracellular staining using Foxp3/Transcription Factor Staining Buffer Set from eBioscience). LN and spleen were stained in a total volume of 100 µl, lung samples in 200 µl. To reduce unspecific antibody binding, surface and intracellular staining were performed in the presence of anti-CD16/CD32 (2.4G2, BioXCell) antibodies and ChromPure rat IgG whole molecule (Jackson ImmunoResearch, West Grove, PA, USA), respectively, and using pre-determined optimal antibody dilutions. Carboxyfluorescein succinimidyl ester (CFSE) staining (10 µM) was performed at 2 x 10^7 cells/ml of PBS for 2 min and 45 sec at room temperature. Reaction was stopped by adding a 10-fold volume of cRPMI (see “Buffers and Solutions”) followed by two centrifugation steps in cRPMI.

5.2.6. Suppression Assay

Naïve CD4 T cells were pre-enriched from murine spleens by magnetic sorting using anti-CD4 microbeads (Miltenyi, Bergisch Gladbach) labeling followed by positive selection using an autoMACS (Miltenyi), as described by the manufacturer. Pre-enrichment was followed by fluorescence-activated cell sorting (FACS) with the target cells having the phenotype of single $CD90.2^{+}CD4^{+}CD62L^{high}CD44^{-}CD25^{-}$ events. 2 x 10^5 CFSE-labeled naïve CD4 T cells were incubated in cRPMI in 96-wells plates for 4 days at 37 °C, >95 % humidity and 5 % CO_2 in the presence or absence of plate-bound 0.5 µg/ml anti-CD3 and 0.1 µg/ml anti-CD28 antibodies (145-2C11 and 37.51, both from eBioscience). Mono-MDSC from spleens or digested lungs of IAV-infected mice were FACS-sorted as single $CD3^{-}CD19^{-}CD49b^{-}CD11b^{+}Ly6C^{++}Ly6G^{-}$ events and added to the cultures at different ratios. 500 µg/ml L-NMMA, 200 µM 1-MDT (both from Sigma-Aldrich) and 500 µg/ml NOR-NOHA (Merck/Calbiochem), were used to block NOS, IDO and arginase, respectively.

5.2.7. Flow cytometry data acquisition

Data was acquired on either BD LSR II SORP or Fortessa and cells were sorted with help of a FACSAria II, all using BD FACSDiva software (all BD Biosciences). Data were analyzed by means of FlowJo software (Treestar, Ashland, OR, USA). Only single cells were considered for flow cytometry analysis. Absolute cell numbers were calculated using a BD Accuri C6 (BD Biosciences) flow cytometer according to instructions by the manufacturer.

5.2.8. Histology

At day 14 of infection, IAV-infected animals were sacrificed and the lungs were excised, gently instilled and subsequently fixed in 4 % buffered formalin (pH 7.2). Following sample preparation was performed in the lab of Dr. Silke Glage (Experimental Pathology, Hannover Medical School, Hannover). After trimming according to the Registry of Industrial Toxicology Animal-data recommendations [115], and dehydration (Shandon Hypercenter, XP), the lungs were embedded in paraffin. Sections were deparaffinized with xylene

and H&E stained to evaluate general morphology by light microscopy (Axioskop 40; Zeiss, Jena). Dr. Silke Glage used a blinded, semi-quantitative scoring-system to grade the pathologic changes in the lungs, as described previously [116].

5.2.9. Enzyme-linked immunosorbent assay (ELISA)

The mouse IFNγ ELISA MAX Deluxe kit was purchased from BioLegend. Measurements were performed as described by the manufacturer. Briefly, lungs were isolated and stored in 1 ml sterile PBS at -70 °C until homogenized. For homogenization, samples were thawed, diluted in 4 ml sterile PBS containing cOmplete™ Protease Inhibitor Cocktail from Millipore (used as described by manufacturer) and processed using a Polytron PT1200C homogenizer (Kinematica, Lucerne, Switzerland). After a centrifugation step for 10 minutes at 1000 g and 4 °C, supernatants were stored at -70 °C until measurement.

5.2.10. Statistics

The following calculation of p-values was performed by Prof. Dr. Frank Klawonn (Department of Bioinformatics and Statistics, HZI) and applied to the comparison of the effect of DT treatment on different immune cell subsets in wildtype and DEREG mice. Log2 Laplace corrected values were considered, i.e. 1 was added to each of the original values and then the logarithm was calculated. The Laplace correction was necessary because there are zero values for which the logarithm is not defined. Under the assumption that the wildtype values followed roughly the same distribution over the whole period of time, the wildtype values were taken as an empirical distribution (most of the wild type value distributions did not resemble a normal distribution). The smallest value of the available DEREG values at time point *t* was considered. When there are *n* DEREG values available at time point *t*, the *p*-value is the probability that a random sample of size *n* from the wildtype values over the whole time period contains only values greater than or equal to the minimum of the considered DEREG values. Using GraphPad Prism software (La Jolla, CA, USA), one tailed, Mann-Whitney test was applied to calculate the *p*-value

when comparing iNOS expression by lung mono-MDSC in mice infected with IAV and either injected with IgG control or anti-IFNγ antibody. * = $p < 0.05$.

6. Results

6.1. Tregs and their role in keeping immune homeostasis

6.1.1. LN and spleen exhibit differences in T cell subset composition in the steady state as well as after Treg depletion

In order to investigate the mechanisms contributing to Treg homeostasis in the steady state, the ratio of Tregs to Tnaïves in LN (pool of inguinal, brachial, axillary, submandibular and cervical LN) and spleen of healthy adult mice was assessed. The ratio of Tregs to Tnaïves was higher in spleen than in LN (Fig. 3A ”homeostasis”). T cell homeostasis requires survival factors such as weak T cell receptor engagement and signaling by cytokines like IL-2 and IL-7. Such ”tonic” signals lead to T cell proliferation without causing full T cell activation and differentiation [117]. The early activation marker CD69 was analyzed here to identify such proliferating T cells and the term activated T cells will be used for this particular $CD69^+$ T cell subset throughout this study. The percentages of $CD69^+$ Tregs and Tnaïves were found to be higher in LN than in spleen (Fig. 3A “homeostasis”, blue rectangles). Next, DEREG mice were used to monitor T cell dynamics after Treg depletion. DEREG mice carry a bacterial artificial chromosome encoding a fusion protein of diphtheria toxin (DT) receptor and enhanced green fluorescent protein under control of the *foxp3* gene regulatory elements, allowing selective $Foxp3^+$ Treg ablation *in vivo* via DT injection [111]. An almost complete depletion of Tregs was achieved two days after a single DT administration (Fig. 3A “d2”). The Treg rebound as well as CD69 expression on T cell subsets were analyzed in LN and spleen on days two, seven and 21 after DT injection (Fig. 3A). The fraction of $CD69^+$ Tnaïves was increased in comparison to homeostatic conditions and remained elevated, particularly in the spleen, at least until day 21 (Fig. 3A, blue rectangles). Surprisingly, the total Tnaïve population expanded in LN but shrunk in spleen within two days after DT application (Fig. 3B). Interestingly, the Treg population exhibited a pronounced overshoot in both organs on day seven after DT (Fig. 3B). In summary, LN and spleen show organ-specific ratios of Tregs to Tnaïves under homeostatic conditions as well as organ-specific Tnaïve dynamics after Treg depletion.

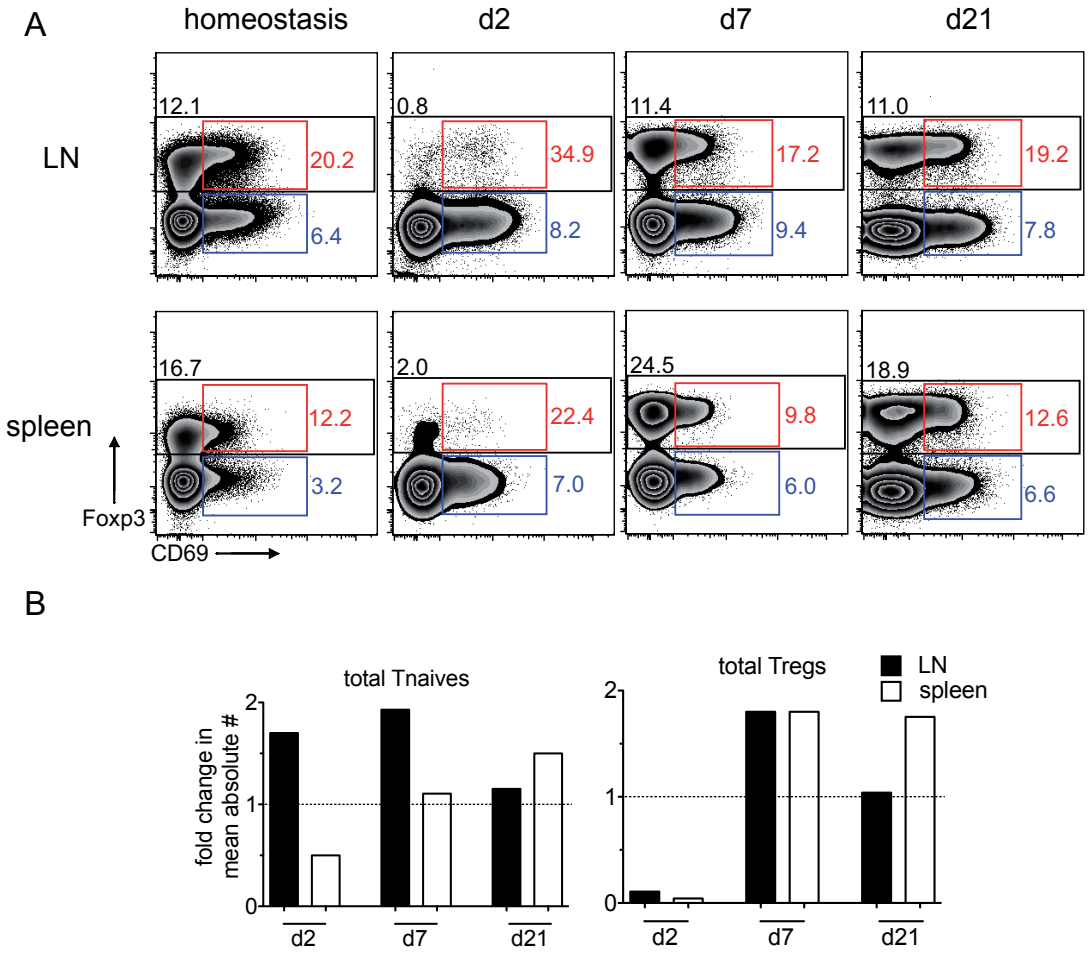

Figure 3: LN and spleen exhibit differences in T cell subset composition in the steady state as well as after Treg depletion.

A: In left panels are zebra plots representing total Tregs (Foxp3$^+$, black rectangles), CD69$^+$ Tregs (red rectangles) and CD69$^+$ Tnaïves (blue rectangles) in LN or spleen in homeostasis. Plots are gated on CD3$^+$CD4$^+$ live singlets. Percentages of Tregs and Tnaïves were calculated among all Tregs and all Tnaïves, respectively, and represent mean values for 14 animals. Other panels show the corresponding data on days two, seven and 21 after DT injection in DEREG mice. Representative data are depicted. *B*: Data on fold change in the mean absolute numbers of total Tnaïves and Tregs on respective days after DT treatment are shown in comparison to PBS-treated DEREG mice (dotted line). Data were pooled from at least two independent experiments (n ≥ 4 for each time point).

6.1.2. A multi-organ mathematical model of T cell homeostasis

The differences observed between LN and spleen in Treg homeostasis and Tnaïve dynamics after Treg depletion might be due to different contributions of homeostatic mechanisms to Treg reconstitution in both organs. To answer this question, the *in vivo* data described above were analyzed with the help of

a specifically designed mathematical model, which was created in co-operation with Prof. Dr. Michael Meyer-Hermann. LN and spleen were modeled as separated entities and recirculation between them was included. This led to the first multi-organ mathematical model for Treg homeostasis and Tnaïve recirculation in mice (Fig. 4). The model incorporates thymic output, apoptosis and proliferation of Tnaïves and Tregs, as well as conversion of Tnaïves to pTregs, allowing the determination of the relative contribution of these different mechanisms to Treg homeostasis. The most important assumptions of the model are:

- Considered organs are thymus, LN, and spleen. LN and spleen embed each Tnaïves and Tregs, both of which can be in a resting or activated state.
- Cells behave according to the same mechanisms in LN and spleen. The organ-specific environment is reflected in the differences in the steady state populations.
- Homeostatic division of Tnaïves is controlled by Tregs through competition for survival factors such as antigen presenting cells, IL-2 and IL-7 [118-120].
- Homeostatic division of Tregs specifically depends on IL-2 provided by homeostatically dividing Tnaïves [121; 122].
- Resting Tnaïves and Tregs migrate between both organs. Migration dynamics are organ-specific, but not T cell subset-specific.
- Mechanisms potentially contributing to Treg reconstitution after depletion are dynamic thymic output, Treg division, and conversion of Tnaïves to Tregs.
- For reasons of simplification, Treg subsets were not considered.

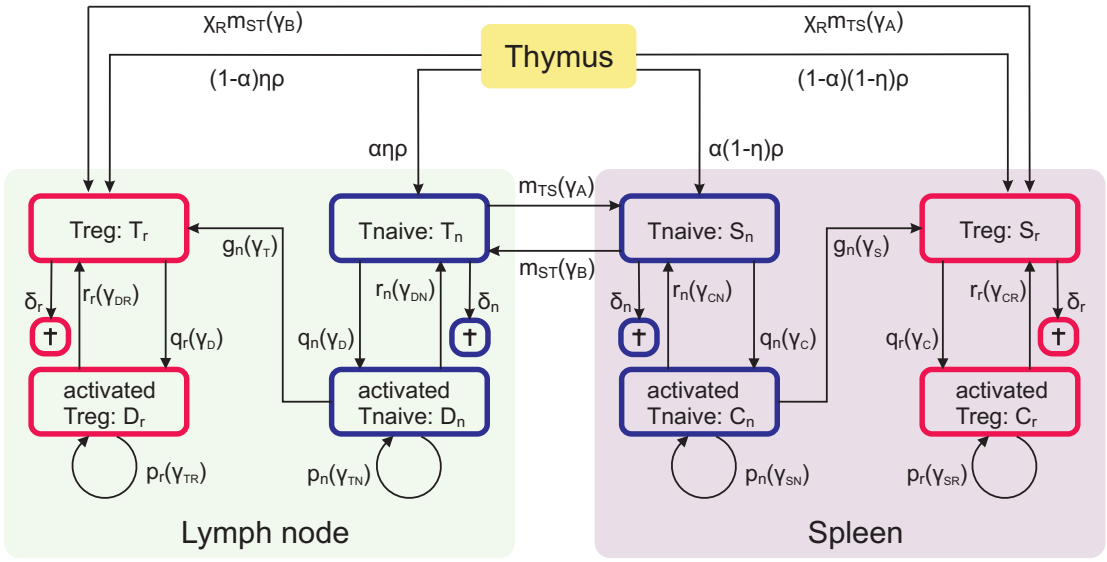

Figure 4: A multi-organ mathematical model of T cell homeostasis.

The thymus generates Tnaïves and Tregs, which both distribute to LN and spleen. Tnaïves and Tregs can undergo apoptosis, become activated and divide, as well as return to the resting state in both organs. Activated Tregs modulate Tnaïve activation, while activated Tnaïves modulate Treg activation. Activated Tnaïves can convert into Tregs. Resting T cells migrate between both organs.

6.1.3. The mathematical model describes Treg reconstitution and Tnaïve dynamics after Treg depletion

The evident question was whether the model could describe the organ-specific differences observed after Treg depletion. As data with high temporal resolution improve the accuracy of parameter prediction, additional experimental Treg depletions were performed. The following time points were included: every six hours until day two, daily until day eight and on days 10, 14, 21 and 60. PBS-treated DEREG mice were taken as baseline. After the fitting routine using a differential evolution algorithm, which was performed by Prof. Dr. Michael Meyer-Hermann, the mathematical model was able to simultaneously describe the measured Treg reconstitution and Tnaïve dynamics in LN and spleen after Treg depletion (Fig. 5). Interestingly, the overshoot of Tregs observed *in vivo* was also reproduced *in silico* (Fig. 5A and B). The quantitative differences in the measured homeostatic populations (Fig. 3A “homeostasis”) turned out to be sufficient to reflect the specificities of LN and spleen. Thus, the qualitatively different behavior in LN and spleen did not require a differentiation of mechanisms between organs. However, for the

mathematical model to describe the *in vivo* data, it was required to assume that Tnaïves dynamically recirculate between the organs as well as that emigration of Tnaïves from LN or spleen is suppressed by the local presence of Tregs. In the model it was assumed that the motility of Tnaïves depends on the ratio of Tregs to Tnaïves. While the exact structure of this dependency was not compulsory, an impact of Tregs onto Tnaïve motility was required in order to reproduce the dynamics of Treg reconstitution. In particular, this was the only identified explanation for the reduction of total T cell numbers in spleen which was accompanied by an increase of total T cell numbers in LN.

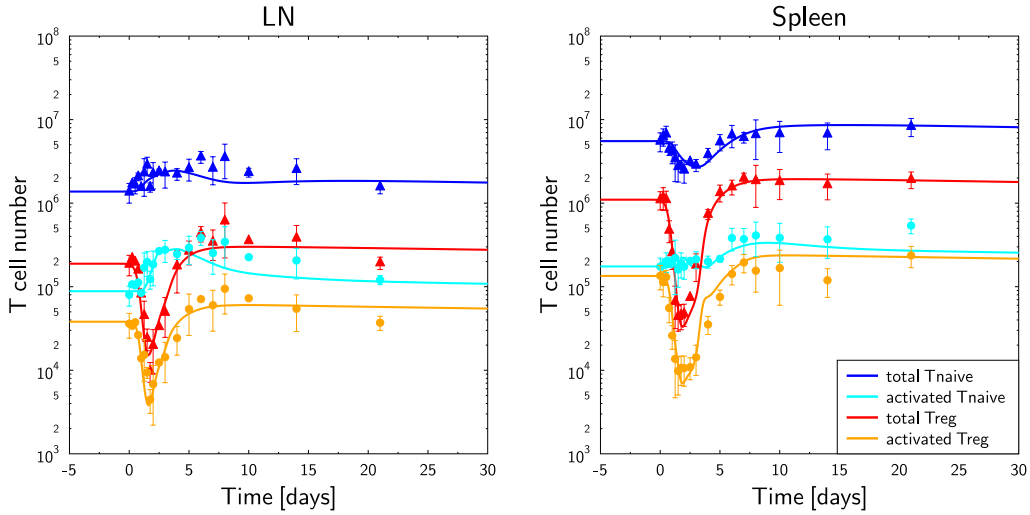

Figure 5: The mathematical model describes Treg reconstitution and Tnaïve dynamics after Treg depletion.

Depletion of Tregs by DT administration (at time zero) and dynamics of reconstitution of the indicated T cell populations are shown in DEREG mice (symbols) and *in silico* (lines). Absolute T cell numbers are shown for LN and spleen. *In vivo* data are pooled from at least two independent experiments as well as two to four animals per time point. *In silico* parameter values were derived from steady state conditions as well as from independent experimental constraints. A best fit of unknown parameters to the *in vivo* data was generated with the help of a differential evolution algorithm.

6.1.4. Blockade of protein synthesis leads to rapid downregulation of CD122 in Tregs

The high affinity IL-2 receptor, which plays a fundamental role in keeping peripheral Treg homeostasis [19; 20], is composed of three subunits: CD25, CD122 and CD132. CD122 is important for the IL-2/CD25 dimeric complex to interact with CD132 as well as for signal transduction [123]. Therefore, the

expression of CD122 by Tregs was followed in the depletion experiments with high temporal resolution described above. Virtually all Tregs in both LN and spleen expressed CD122 in the steady state (Fig. 8, “PBS”, data from LN are shown). Surprisingly, although the number of Tregs found in LN and spleen only started to decrease 18 hours after DT application into DEREG mice (Fig. 5), a substantial downregulation of CD122 from the surface of Tregs was observed already six hours after treatment (Fig. 6). In other words, although Tregs were still physically present in LN and spleen in the first hours after treatment, DT, which acts in eukaryotic cells unsettling protein synthesis, had already started disrupting Treg homeostasis at the cellular level. Tregs showed normal expression of CD122 during rebound at later time points (data not shown).

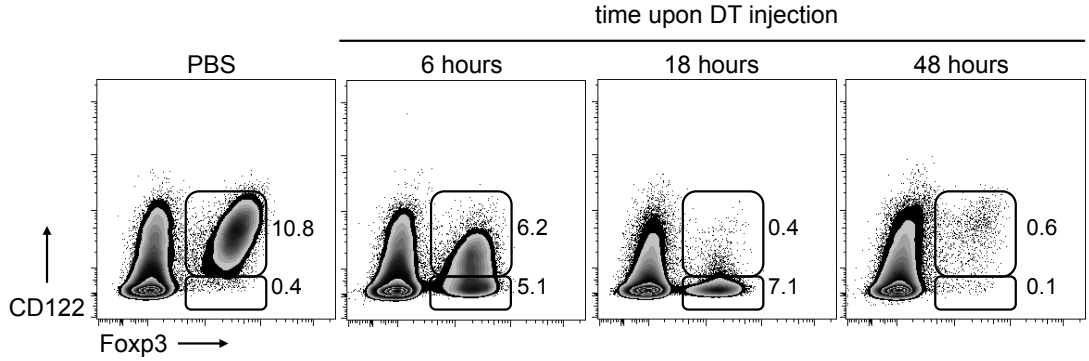

Figure 6: Blockade of protein synthesis leads to rapid downregulation of CD122 in Tregs.

Zebra plots show expression of CD122 and Foxp3 in gated $CD3^+CD4^+$ single events from LN of DEREG mice after treatment with PBS or DT at indicated time points. Balloons represent gates and numbers are percentages of cells within gates. Representative data from two experiments each with two mice per time point are shown.

6.1.5. Recirculation of Tregs is decreased when compared to Tnaïves

The model allows for T cell recirculation of both Tnaïves and Tregs, whereby the migration of Tregs is controlled by the parameter χ_R. For $\chi_R = 1$, Tregs and Tnaïves recirculate at the same rates. The existence of a steady state solution based on the measured T cell subsets in the resting state imposes $\chi_R < 0.25$. Thus, the model predicts that recirculation of Tregs is reduced in

comparison to Tnaïves. When χ_R was included in the parameter fitting routine, the differential evolution algorithm determined a value of $\chi_R = 0.0036$. As this value was very small, only the results where recirculation of Tregs was neglected are presented. However, all results were repeated with $\chi_R = 0.2$ and the quality of the best fit was the same as without Treg recirculation and the statements derived from the model remained unaltered (data no shown). However, recirculation of T cells became asymmetric, as cells only migrated from spleen to LN but not back and the steady state frequency of trans-organ migration was very low, in contradiction to measured organ transition times of T cells [124-126]. This result indicates that, in comparison to Tnaïves, Tregs recirculate at a much lower rate.

6.1.6. Conversion added an important contribution to Treg homeostasis, especially in LN

Conversion of Tnaïves to pTregs is considered an essential process for complementation of the Treg repertoire towards recognition and tolerance of non-self antigens. It was therefore of interest to estimate the rate of peripheral Treg conversion *in vivo*. Using another mouse strain in which it is also possible to deplete Tregs by DT injection, Suffner et al. described that proliferation of Tregs is the dominant path of Treg reconstitution [127]. Although the results here are in agreement with that (Fig. 7, red lines), the present analysis went beyond and asked to which extent conversion of Tnaïves into pTregs happens and which role it plays in Treg reconstitution after depletion. Indeed, very high levels of conversion following Treg depletion were found (Fig. 7A and B, green lines), ranging from 1×10^5 pTregs appearing per day in spleen to 2×10^5 in LN, at the peak of conversion. Even more importantly, conversion peaked in both organs at day two after DT injection, while Treg proliferation peaked one to two days later (Fig. 7A and B, red lines). These results suggest that conversion of Tnaïves into pTregs triggers reconstitution of the Treg population. Indeed, without this early conversion, the Treg population would not acquire the critical mass enabling a fast rebound of Tregs within three days after their disappearance following DT treatment.

The next question was whether conversion plays a relevant role also in Treg homeostasis under steady state conditions. In the resting state, maintenance of LN Tregs equally depended on conversion, thymic output and proliferation (Fig. 7A, compare green, black and red lines at time points before zero), whereas conversion had a lower contribution to splenic Tregs in comparison to thymic output and proliferation (Fig. 7B). According to the model, around 2400 and 760 converted pTregs appeared per day in LN and spleen in the steady state, respectively.

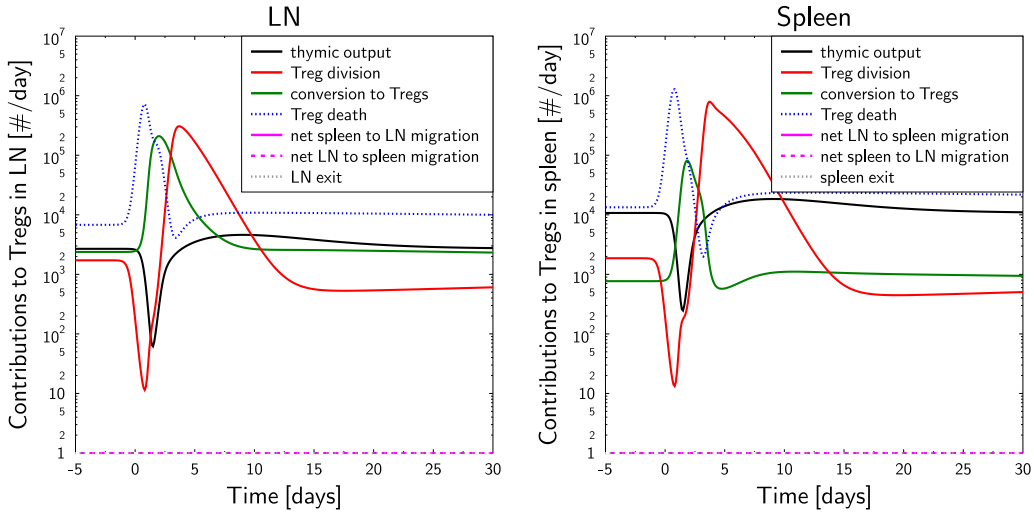

Figure 7: Conversion added an important contribution to Treg homeostasis, especially in LN.

The contributions to the reconstitution of the Treg population after depletion are shown in LN and spleen: thymic output (black line), Treg division (red line) and conversion from Tnaïve to Treg (green line) as well as of cell death (dotted blue line, multiplied with 1 for comparison). The respective contributions correspond to the terms contributing to total Treg compartments.

If there is a higher conversion rate in LN compared to spleen, this should induce a larger fraction of pTregs in LN. Recently, tTregs but not pTregs were shown to express Nrp1 at steady state [30; 31]. Using Nrp1 staining for flow cytometry, the percentage of Tregs lacking the expression of Nrp1 in LN and spleen was determined. A slightly higher percentage of Nrp1$^-$ pTregs was found in LN in comparison to spleen (27.7 ± 5.0 % in LN and 20.9 ± 2.9 % in spleen, n = 7, Fig. 8), which is overall in line with the *in silico* results. In summary, conversion added an important contribution to Treg homeostasis,

especially in LN.

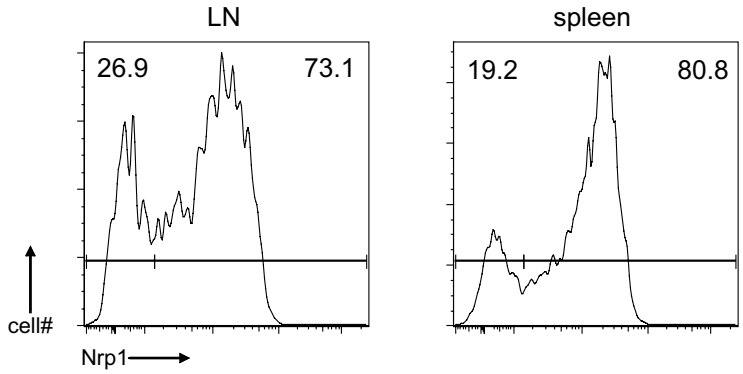

Figure 8: Percentage of Foxp3$^+$Nrp1$^-$ pTregs slightly differs in LN and spleen.
Histograms show Nrp1 expression on Tregs in LN and spleen. Cells were gated as CD3$^+$CD4$^+$Foxp3$^+$ live singlets. Representative data of seven mice from two independent experiments are shown.

6.1.7. Total number of leukocytes increases in LN but not in spleen upon Treg depletion

In the experiments described above, it was shown that Tnaïves and Tregs display different responses to Treg depletion in LN and spleen. For example, the number of Tnaïves decreased in spleen but increased in LN. The next interesting point was to verify whether other immune cell subsets also show differential responses when comparing their LN and spleen populations after Treg depletion. Indeed, important changes in the total number of cells were observed only in LN but not in the spleen (Fig. 9). The leukocyte number dramatically increased within four to six days of Treg depletion in LN, with the peak of accumulation being observed between days six and eight. The number of cells returned to normal levels 60 days after DT injection. That means, although the Treg population achieves homeostatic levels again just a few days after depletion (Fig. 9), a disturbance in the total leukocytes population of LN lasting for several weeks was observed.

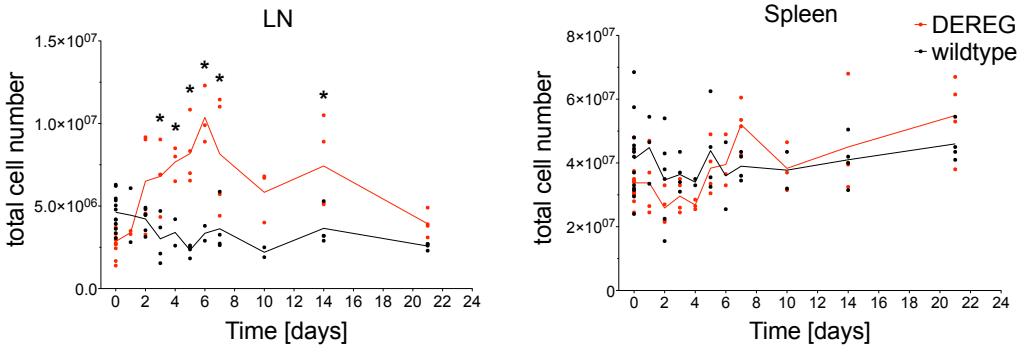

Figure 9: Total number of leukocytes increases in LN but not in spleen upon Treg depletion.

Left and right panels show the total number of leukocytes in LN and spleen, respectively. Mice were treated with DT at day zero. Red symbols show data from DEREG mice while black symbols show data from wildtype mice. Values for individual mice (circles) as well as lines connecting means are plotted. Data were pooled from at least two independent experiments per time point. * = $p < 0.05$ at indicated time point.

A range of immune cell subsets is present in LN and spleen in the steady state and the next question was which of them change in numbers upon Treg depletion. Thereto, multicolor flow cytometry and different antibody combinations were applied to analyze immune cell composition in LN and spleen of treated mice. The gating strategy is shown in Figure 10. NK cells (Fig. 10A), B cells (Fig. 10B), DC, monocytes and neutrophils (Fig. 10C) could be distinguished. The next step was to use multicolor flow cytometry to determine the kinetics of each of these populations in LN and spleen after Treg ablation.

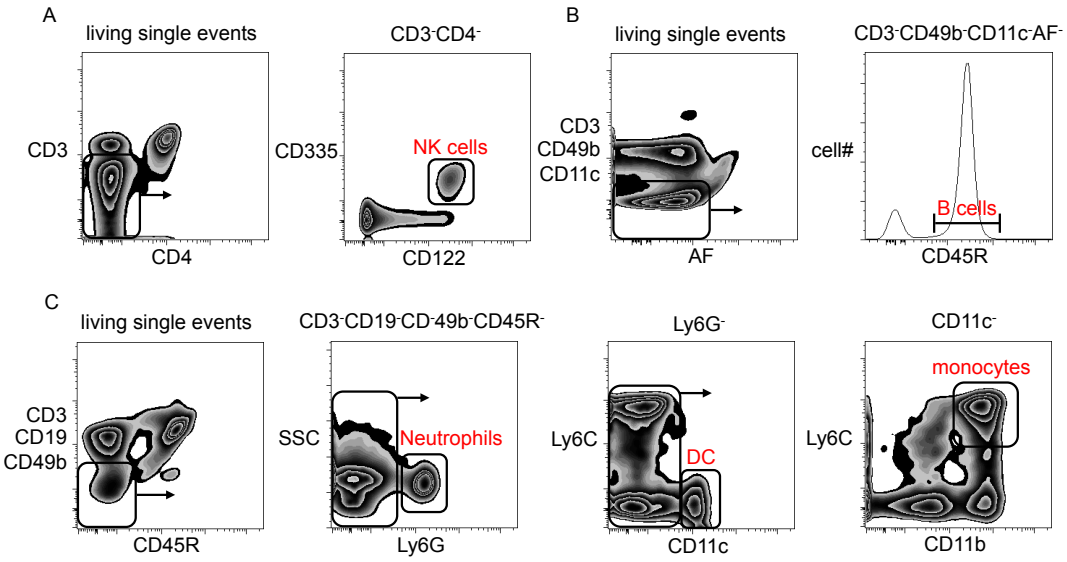

Figure 10: Multicolor flow cytometry allows for characterization of the response of a range of immune cell subsets to Treg depletion.

Balloons represent gates and arrows denote when further gating was performed. *A*: living single events were gated for lack of CD3 and CD4. NK cells were defined as $CD3^-CD4^-$ events expressing CD335 (NKp46) and CD122. *B*: living single events were gated for the absence of CD3, CD49b, CD11c and autofluorescence (AF). After that, expression of CD45R (B220) was used to define B cells. *C*: living single events lacking CD3, CD19, CD49b and CD45R were gated. After that, neutrophils were defined as $Ly6G^+$ events. $Ly6G^-$ events were further analyzed based on the presence (DC) or absence of CD11c. Events lacking CD11c but expressing both CD11b and high levels of Ly6C were defined as monocytes.

6.1.8. DC and NK cells transiently accumulate in the LN and spleen upon Treg depletion.

The first immune cell subsets analyzed were the DC and NK cell populations, which are controlled by Tregs under homeostatic conditions. Tregs keep homeostasis of the DC population via a Flt3-dependent mechanism [44; 45] and restrain NK cell numbers by consumption of T cell-produced IL-2 [47-49]. In this study, the splenic populations of both DC and NK cells only slightly and transiently increased in absence of Tregs, whereas LN DC and NK cells became notably more numerous after Treg depletion (Fig. 11). Interestingly, the increase in NK cells seemed to anticipate the increase in DC in both organs, with LN NK cells achieving high levels already on day 3 but LN DC only on day 4. The decline in both cell populations was comparable, starting on day 6. Therefore, Treg depletion seems also to differentially influence DC

and NK cells when comparing their LN and spleen populations.

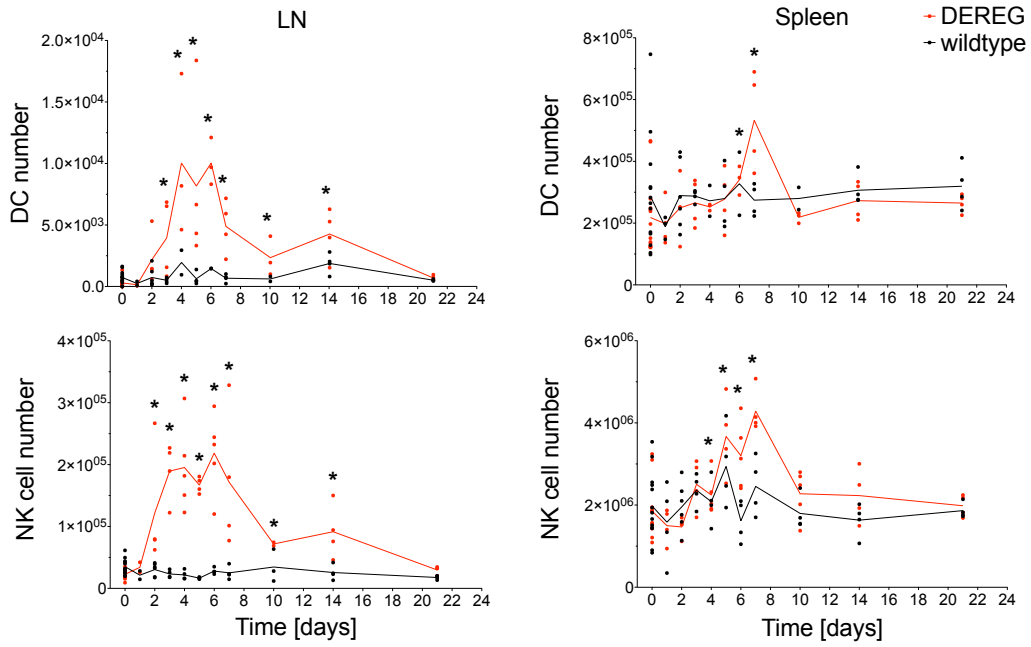

Figure 11: DC and NK cells transiently accumulate in the LN and spleen upon Treg depletion.

Left and right panels show the number of indicated cell populations in LN and spleen, respectively. Upper panels show data for DC, lower panels for NK cells. DEREG mice (red) and wildtype littermates (black) were treated with DT at day zero. Values for individual mice (circles) as well as lines connecting means are plotted. Data were pooled from at least two independent experiments per time point. * = $p < 0.05$ at indicated time point.

6.1.9. mo-DC appear punctually in LN upon Treg depletion

Inflammation induces monocyte differentiation into antigen-presenting cells, so called mo-DC [128]. mo-DC, which are characterized by the expression of CD11b and intermediate to high levels of Ly6C and CD11c, are completely absent from LN in the steady state (Fig. 12, left panel). Neither before nor after treatment mo-DC were found in the spleens (data no shown). Interestingly, a population of $CD11b^{+}Ly6C^{+}CD11c^{+}$ cells appeared in LN upon Treg depletion (Fig. 12). The accumulation of mo-DC in LN of Treg-depleted mice started at day 2, with sharp increase up to day 4 and a rapid decrease afterwards (Fig. 12). Hence, Treg depletion led to a transient accumulation of mo-DC in LN.

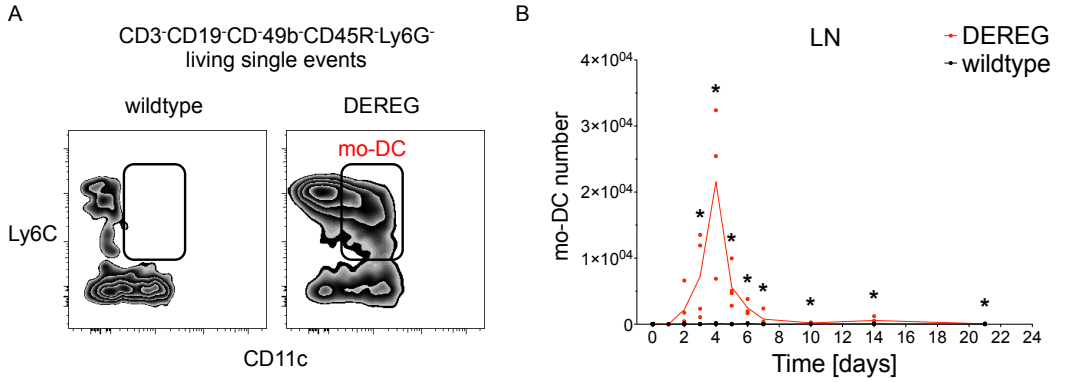

Figure 12: mo-DC appear punctually in LN upon Treg depletion.

A: gating strategy for mo-DC on day four upon DT is shown. *B*: the numbers of mo-DC in LN are plotted. DEREG mice (red) and wildtype littermates (black) were treated with DT at day zero. Values for individual mice (circles) as well as lines connecting means are plotted. Data were pooled from at least two independent experiments per time point. * = $p < 0.05$ at indicated time point.

6.1.10. B cells accumulate for at least three weeks in LN but not in the spleen upon Treg depletion

Tregs were shown to be involved in the control of antigen-specific B cell responses [50; 51]. Further, defective B cell anergy as well high titers of autoantibodies are found in Foxp3-deficient mice [52; 129]. As seen in Figure 13, there was a considerable and long-lasting increase in the numbers of B cells in LN in the absence of Tregs, while no differences were observed in the spleen. The increase in the B cell population in LN, which represents the third largest cell population in this organ, might be responsible for the augmented total number of cells observed in LN upon Treg depletion (Fig. 9). Although one could expect an increased incidence of autoimmunity in mice with such an expansion in the B cell population within LN, which is potentially producing self-reactive antibodies, no apparent signs of autoimmunity were detected in these mice even 60 days after Treg depletion (data not shown).

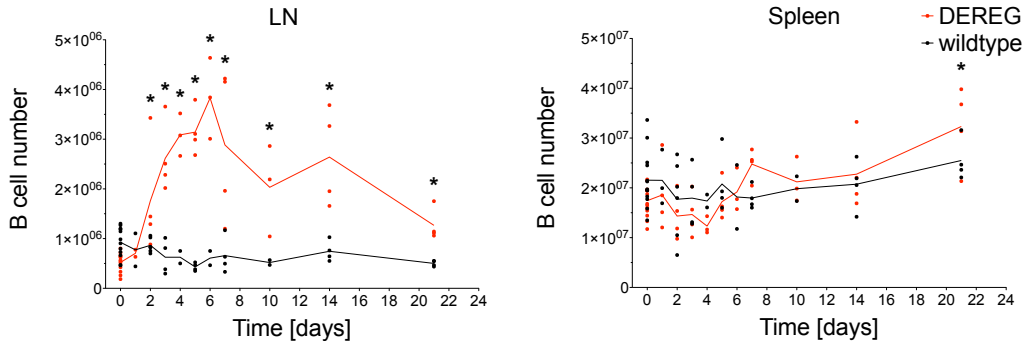

Figure 13: B cells accumulate for at least three weeks in LN but not in the spleen upon Treg depletion.

Left and right panels show the number of B cells in LN and spleen, respectively. DEREG mice (red) and wildtype littermates (black) were treated with DT at day zero. Values for individual mice (circles) as well as lines connecting means are plotted. Data were pooled from at least two independent experiments per time point. * = $p < 0.05$ at indicated time point.

6.1.11. $CD11b^{+}Ly6C^{+}Ly6G^{+}$ and $CD11b^{+}Ly6C^{++}Ly6G^{-}$ cells transiently accumulate in both LN and spleen upon Treg depletion

On one hand, DT injection in DEREG mice leads to systemic death of Tregs. Hence, an accumulation of phagocytic cells, including neutrophils and monocytes, in Treg-depleted mice should be expected. On the other hand, the lack of autoimmunity in Treg-depleted DEREG mice makes it tempting to speculate whether other immune regulatory cells might be responsible for immune modulation in the absence of Tregs. A candidate population for this are MDSC, which have the ability to suppress immune responses [54; 55]. The numbers of LN and spleen $CD11b^{+}Ly6C^{++}Ly6G^{-}$ and $CD11b^{+}Ly6C^{+}Ly6G^{+}$ cells, which are neutrophils and monocytes in the steady state but also include mono-MDSC and PMN-MDSC in certain types of inflammation, were determined. Indeed, there was an increase in both populations in LN and spleen after DT application in DEREG mice (Fig. 14). Consequently, Treg depletion led to an accumulation of cells which might be phagocytic myeloid cells, but might also include cells with suppressive activity, exerting immune regulation once Tregs are missing. Notably, wildtype littermates receiving DT also showed a rapid but short increase in spleen neutrophils (Fig. 14, black line of lower right), which might be due to minor contamination of DT with

some bacterial products.

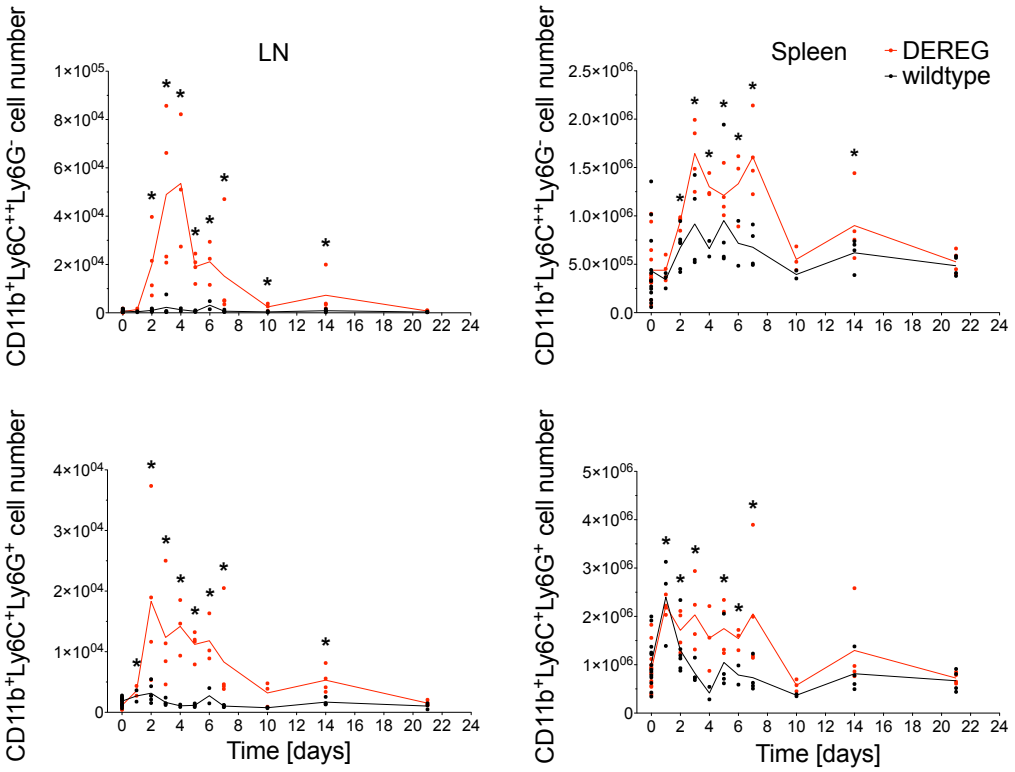

Figure 14: CD11b$^+$Ly6C$^+$Ly6G$^+$ and CD11b$^+$Ly6C^{++}Ly6G$^-$ cells transiently accumulate in both LN and spleen upon Treg depletion.

Left and right panels show the number of indicated cell populations in LN and spleen, respectively. Upper panels show data for CD11b$^+$Ly6C^{++}Ly6G$^-$ cells, lower panels for CD11b$^+$Ly6C$^+$Ly6G$^+$ cells. DEREG mice (red) and wildtype littermates (black) were treated with DT at day zero. Values for individual mice (circles) as well as lines connecting means are plotted. Data were pooled from at least two independent experiments per time point. * = $p < 0.05$ at indicated time point.

In the first part of this study, Treg homeostasis as well as their role in keeping immune balance was investigated. In summary, the relative contributions of different mechanisms to Treg homeostasis in mice were investigated, showing that they quantitatively differ in LN and spleen. These findings are supported by the first multi-organ mathematical model of Treg homeostasis and Tnaïve recirculation in mice, created in co-operation with Prof. Dr. Michael Meyer-Hermann. Further, it was examined how immune cell subsets such as B cells, NK cells and myeloid cells respond to the absence of Tregs in LN and spleen, demonstrating that Treg-mediated regulation acts in a

broad immunological context with important differences in LN and spleen

6.2. Role of MDSC in IAV infection

6.2.1. Murine lungs contain cells that express markers of monocytes and mono-MDSC before and after IAV infection

In the second part of this thesis, the aim was to examine the role of MDSC in IAV infection. Monocytes were claimed to be the “necessary evil” of the immune response against IAV. Avoiding their accumulation either genetically or chemically led to an overall improvement in mouse survival [65; 107]. In those studies, monocytes were termed inflammatory cells but their potential differentiation into mono-MDSC was not considered, maybe because MDSC were almost exclusively described in chronic but not in acute viral infection. It was therefore interesting to answer the question whether the mononuclear myeloid cells that accumulate in the lungs upon IAV infection also have a $CD11b^{+}Ly6C^{++}Ly6G^{-}$ phenotype. The lungs of PBS-treated, healthy control mice contained a small population of $CD11b^{+}Ly6C^{++}Ly6G^{-}$ cells (Fig. 15 “d0”), which were likely monocytes. Importantly, $CD11b^{+}Ly6C^{++}Ly6G^{-}$ cells were also found in infected lungs six days upon infection with IAV (Fig. 15 “d6”). Since the existence of cells with this phenotype at inflamed sites was associated with the presence of mono-MDSC, theses findings were interpreted as a first hint that mono-MDSC might indeed accumulate in IAV-infected lungs.

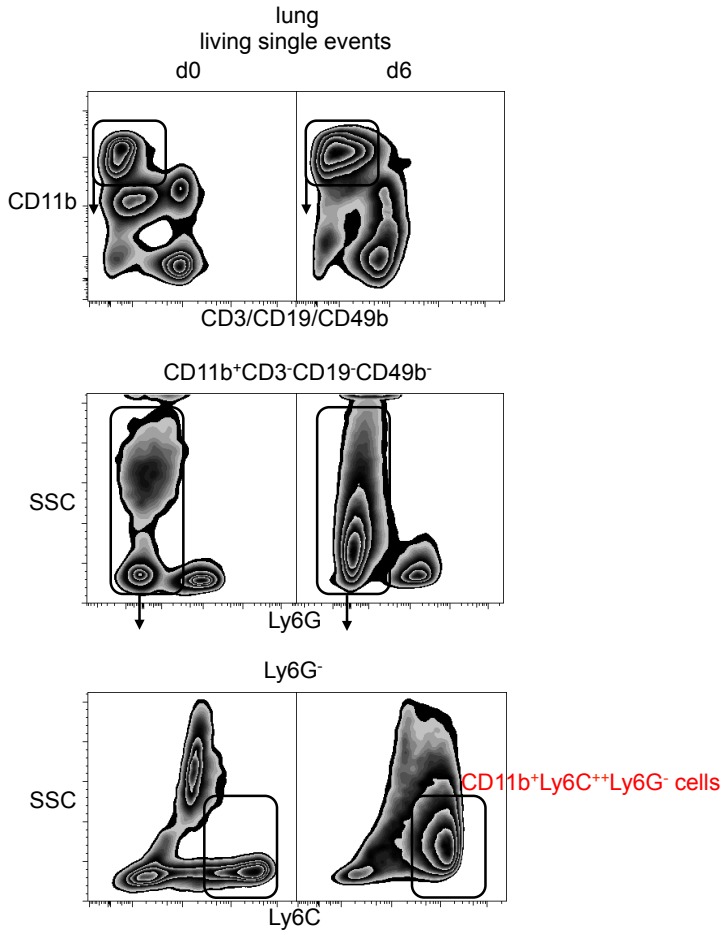

Figure 15: The murine lungs contain cells that express markers of monocytes and mono-MDSC before and after IAV infection.

Panels show the gating strategy for CD11b^{+}Ly6C^{++}Ly6G^{-} cells. Cells were isolated from lungs of PBS-treated (left, d0) mice or IAV-infected mice on day six of infection (right, d6). Top panels were pre-gated on single events after exclusion of dead cells. Plots are representative for two independent experiments each with three to five mice per time point.

6.2.2. CD11b^{+}Ly6C^{++}Ly6G^{-} cells partially express DC maturation and activation markers

Lung-infiltrating monocytes were previously described to mature in the lung and give rise to TiP-DC upon IAV infection [65; 107]. The next step was therefore to determine the phenotype of CD11b^{+}Ly6C^{++}Ly6G^{-} cells before and after infection with regard to the expression of cell markers associated with DC differentiation. Before infection, monocytes expressing CD11c, MHCII or CD86 could hardly be found (Fig. 16, gray shadow). Six days after infection, between 40 % and 50 % of the CD11b^{+}Ly6C^{++}Ly6G^{-} cells found in the lung

expressed MHCII or CD11c (Fig. 16, left and central panels). The expression of CD86 was even more frequent with about 80 % the $CD11b^{+}Ly6C^{++}Ly6G^{-}$ cells expressing this marker (Fig. 16, right panel). Therefore, a part but not all lung $CD11b^{+}Ly6C^{++}Ly6G^{-}$ cells seemed to be mature inflammatory TiP-DC upon IAV infection.

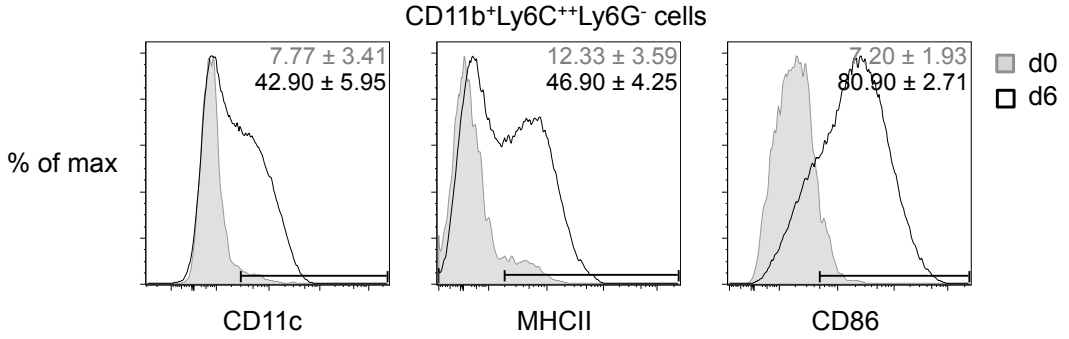

Figure 16: $CD11b^{+}Ly6C^{++}Ly6G^{-}$ cells partially express DC maturation and activation markers.

Panels show expression of CD11c, MHCII and CD86 on lung $CD11b^{+}Ly6C^{++}Ly6G^{-}$ cells pre-gated as in Figure 15. Cells were isolated from lungs of PBS-treated mice (gray shadow) and IAV-treated mice on day six of infection (black line). Numbers denote mean frequency ± standard deviation of gated cells among total $CD11b^{+}Ly6C^{++}Ly6G^{-}$ cells. Data are from representative mice from two independent experiments with a total of three (d0) or four mice (d6).

6.2.3. $CD11b^{+}Ly6C^{++}Ly6G^{-}$ cells isolated from the lung or spleen of IAV-infected mice show suppressive activity

Until now, only a functional assay can prove that $CD11b^{+}Ly6C^{++}Ly6G^{-}$ cells accumulating at sites of inflammation are indeed mono-MDSC. This is due to a lack of surrogate markers that can be used to unambiguously identify them. Therefore the next aim was to assess the functional activity of cells accumulating in infected lungs. $CD11b^{+}Ly6C^{++}Ly6G^{-}$ cells were sorted from the murine lungs or spleens six days upon IAV infection and incubated them with CFSE-labeled Tnaïves *in vitro* in the presence of anti-CD3/anti-CD28 antibodies. This was to test whether IAV mono-MDSC show suppressive activity. $CD11b^{+}Ly6C^{++}Ly6G^{-}$ cells from both organs were able to suppress, at least partially, Tnaïve proliferation (Fig. 17A-B). This result demonstrates that IAV leads to the accumulation of $CD11b^{+}Ly6C^{++}Ly6G^{-}$ cells with a bona fide

mono-MDSC phenotype i.e. with the ability to suppress a T cell response. It also confirms that mono-MDSC can appear during acute virus infection.

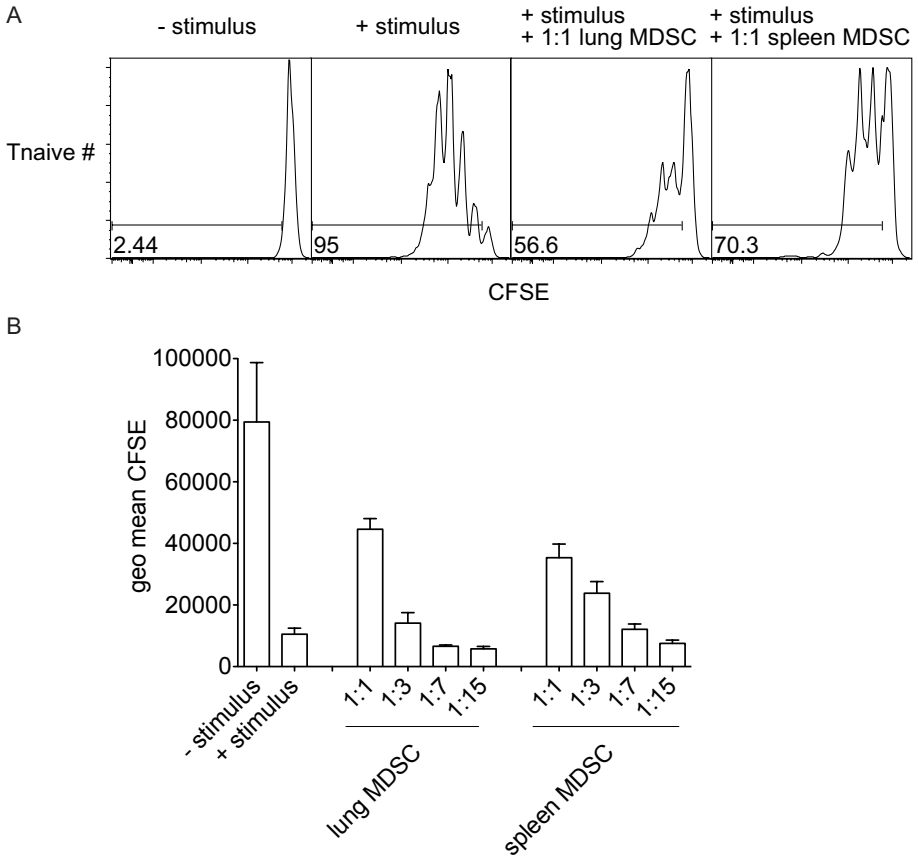

Figure 17: CD11b^{+}Ly6C^{++}Ly6G^{-} cells isolated from the lung or spleen of IAV-infected mice show suppressive activity.

Upper panel shows histograms with dilution of CFSE in Tnaïves (pre-gated as living single CD4^{+}CD11b^{-} cells) incubated for four days either in absence (- stimulus) or presence (+ stimulus) of anti-CD3/CD28 and added mono-MDSC sorted as in Figure 15 from the lungs or spleens of IAV-infected mice at a 1:1 ratio. Numbers show frequency of cells that underwent at least one division. Each condition was performed in triplicates and shown are representative data. Lower panel shows geometric mean fluorescence intensity (geo mean) of CFSE in Tnaïves pre-gated as in upper panel, but with different mono-MDSC:Tnaïve ratios. Data from two independent experiments were pooled.

6.2.4. Peak of mono-MDSC accumulation is followed by an increase in the absolute number of T cells

Mono-MDSC, which show suppressive activity towards T cells, can be found after IAV infection (Fig. 17). The next step was to determine the kinetics of mono-MDSC and T cell accumulation in the lungs of IAV infected mice to

evaluate whether presence of these cell populations overlap *in situ*. On day six after infection, which is also roughly the time when mice start recovering body weight (data not shown), mono-MDSC numbers have already reached their highest levels but only few T helper cells and CTL could be found *in situ* (Fig 17). On day seven, the number of mono-MDSC was similar as on day six and steadily decreased afterwards. Also on day seven, the population of T helper cells achieved its plateau, with similar cell numbers being found until day ten. The CTL population achieved its highest numbers on day eight, which remained stable also on day ten. On day 14, all cell populations were at very low numbers again (Fig 17). Therefore, although mono-MDSC precede T cell accumulation in the lungs, presence of both cell subsets *in situ* overlaps for some days during initiation of the adaptive response. Since animals start regaining body weight in this phase, an indication of effective virus clearance, and since T cells play a determinant role in this phase [130; 131], the results indicates that mono-MDSC do not hamper a proper T cell response to the virus.

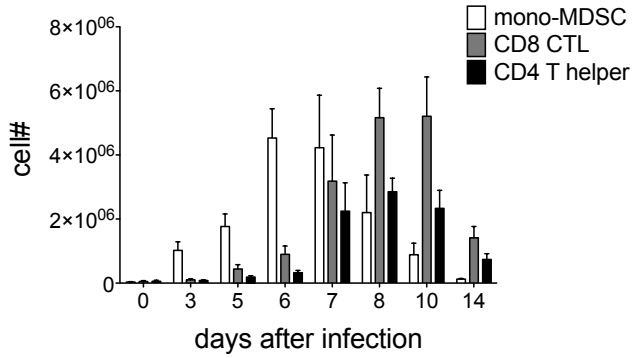

Figure 18: Peak of mono-MDSC accumulation is followed by an increase in the absolute number of T cells.

Bar graph shows the number of total mono-MDSC, $CD8^+$ CTL and $CD4^+$ T helper cells ($CD3^+CD8^+$ and $CD3^+CD4^+Foxp3^-$ single living events, respectively) in the lungs of PBS-treated (d0) or IAV-infected mice on indicated days after infection as determined by flow cytometry. Data were pooled from two independent experiments each with three to five mice per time point.

6.2.5. IFNγ triggers iNOS expression in IAV-induced lung mono-MDSC

IAV induces accumulation of mono-MDSC with suppressive activity towards T

cells (Fig. 17) and the presence of mono-MDSC and T cells overlap for some days in IAV-infected lungs (Fig. 18). A previous study from our group pointed out that the IFNγ/iNOS axis plays a key role in controlling Th1-induced inflammation [132]. Moreover, although iNOS is expressed by TiP-DC at inflamed sites, likely mediating killing of invading pathogens [133], this enzyme is also among the most important effector molecules mediating suppression by MDSC [54]. So, the aim was to determine the kinetics of IFNγ availability in lung tissue as well as iNOS-production by mono-MDSC in IAV-infected lungs during the course of infection. A strong correlation between presence of IFNγ and numbers of iNOS-expressing mono-MDSC in IAV-infected lungs was observed (Fig. 19A and B). IFNγ and iNOS-expressing cells were hardly detectable in lungs until day five of infection. Remarkably, on day six, although only few T helper cells and CTL were found in the IAV-infected lungs (Fig 18) and T cells are the main source of IFNγ during IAV infection [104; 134], the highest amount of IFNγ and the highest number of iNOS-producing mono-MDSC were observed on this day (Fig. 19A and B). Surprisingly, at later stages, when T cells heavily accumulated in the IAV-infected lungs (Fig 18), IFNγ and the number of iNOS-expressing cells steadily decreased and eventually reached normal levels already at day ten (Fig. 19A and B). An *in vivo* injection with a monoclonal anti-IFNγ blocking antibody on day five of infection led to a significant decrease in the number of $iNOS^+$ mono-MDSC one day later (Fig. 19C and D). In contrast to previous observation from our group [132], however, IFNγ neutralization *in vivo* did not change outcome of disease (Fig. 20). When comparing infected mice treated either with isotype control or anti-IFNγ antibody, no differences were observed in loss of body weight and in lung damage (Fig. 20). Hence, a wave of IFNγ availability on day six of infection led to a considerable response by mono-MDSC in the form of iNOS expression. Notably, this kinetics correlates with the initiation of adaptive immunity in the murine model of IAV infection, which starts at around one week after infection and leads to viral clearance [103; 135].

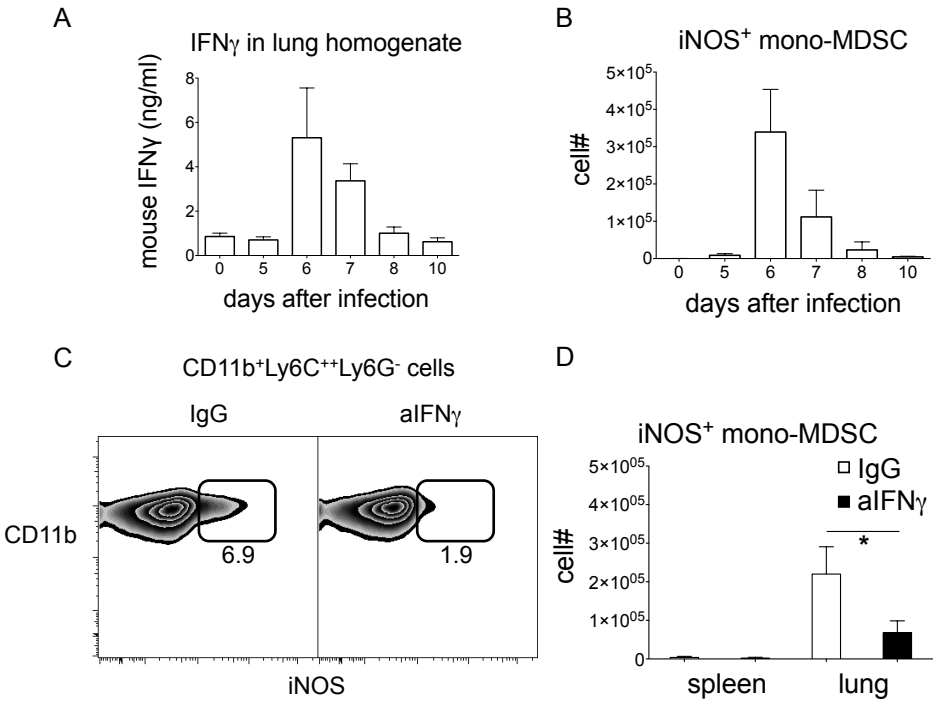

Figure 19: IFNγ triggers iNOS expression in IAV-induced lung mono-MDSC.

A: The concentration of IFNγ in lung homogenate of PBS-treated (d0) and IAV-infected mice on indicated days after infection as determined by ELISA is shown. Lung homogenates from four to six mice per time point from two independent experiments were analyzed in one ELISA experiment. *B*: The number of iNOS-producing mono-MDSC in the lungs of PBS-treated (d0) and IAV-infected mice on indicated days after infection as determined by flow cytometry (iNOS$^+$ events, pre-gated similar as in Figure 15) is shown. Data were pooled from two independent experiments each with three to five mice per time point. *C*: Panels show expression of iNOS by lung mono-MDSC (pre-gated as in Figure 15) from IAV-infected mice on day six after infection and either injected with IgG isotype control (IgG) or anti-IFNγ (aIFNγ) antibody one day before. One representative mouse per treatment from two independent experiments with a total of five (IgG) or seven (aIFNγ) mice are shown. Numbers are percentages of iNOS$^+$ events among mono-MDSC. *D:* Bar graph shows the mean number of iNOS-producing mono-MDSC in the experiments shown in *C*. Data were pooled from both independent experiments. Error bars in all graphs show standard deviation. * = $p < 0.05$.

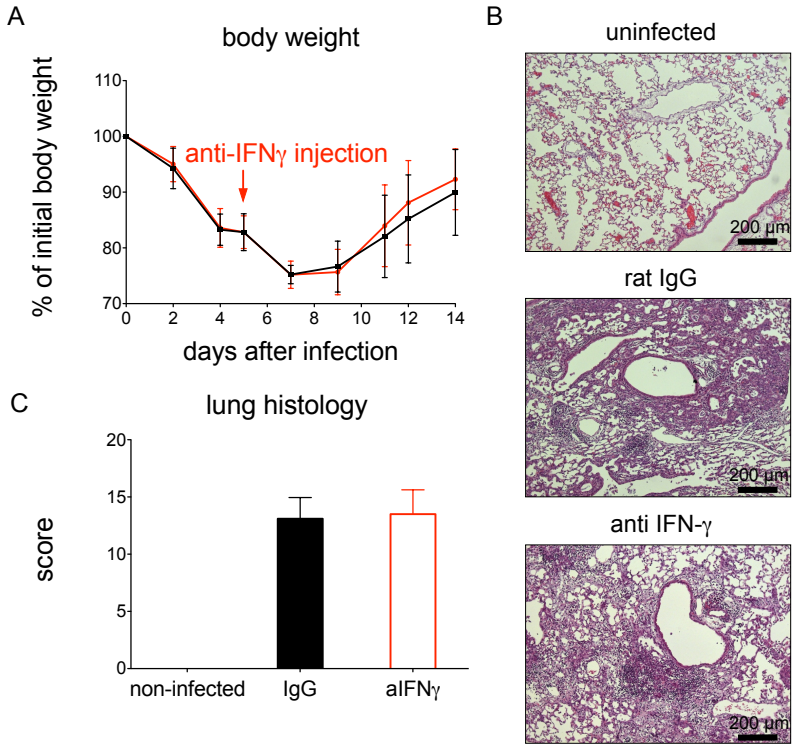

Figure 20: IFNγ blockade during IAV infection does not change disease outcome.
A: mean percentages of initial body weight of IAV-treated mice on different days after infection and either injected with anti-IFNγ (red symbols) or IgG isotype control (black symbols) on day five of infection are shown. *B* and *C*: Mice were sacrificed on day 14 of infection and their lungs isolated for histological analysis. Representative pictures are shown in *B*, the mean clinical scores of mice in different groups are shown in *C*. Error bars show standard deviation. Data in *A* and *C* were pooled from two independent experiments each with five mice per group.

6.2.6. T cell suppression by lung IAV mono-MDSC is not triggered by IFNγ *in vivo*

Previous work from our lab showed an essential role of IFNγ in switching on iNOS expression and, thereby, triggering suppressive activity in MDSC (unpublished data and [132]). Therefore, it was of interest to analyze whether IFNγ is also responsible to elicit suppression of T cell proliferation by mono-MDSC in the lungs of IAV infected mice. Thereto, *in vitro* suppression assays were performed using mono-MDSC isolated from lungs of mice on day six of IAV infection and treated the day before with isotype control or with anti-IFNγ antibody. Although IFNγ neutralization successfully blocked iNOS expression by mono-MDSC (Fig. 19), suppression activity was not different when comparing control and anti-IFNγ-treated groups (Fig. 21). This indicates that

IFNγ is not needed to trigger suppressive activity in mono-MDSC in the lungs of mice infected with IAV.

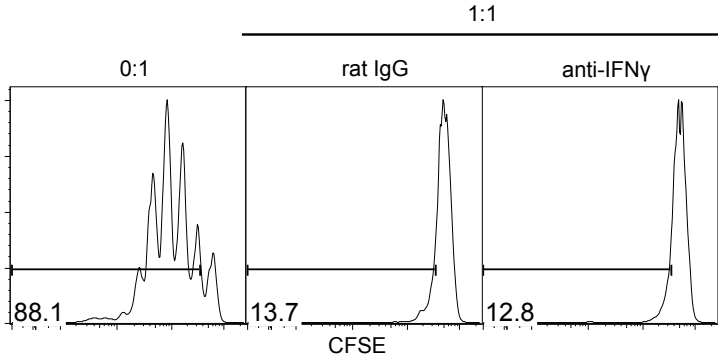

Figure 21: T cell suppression by lung IAV mono-MDSC is not triggered by IFNγ *in vivo*. Histograms show dilution of CFSE in Tnaïves pre-gated and incubated as in Figure 17 but with mono-MDSC being isolated from day six IAV-infected mice either treated with rat IgG isotype control or anti-IFNγ on day before. Numbers show frequency of T cells undergoing at least one division. Each condition was performed in triplicates and representative data are shown. Data from one out of two independent experiments with comparable results are shown.

6.2.7. T cell suppression by lung IAV mono-MDSC is iNOS-dependent

Finally, the aim was to examine the mechanism of suppression of T cell proliferation by IAV-induced lung mono-MDSC. iNOS, Arg1 and IDO, three amino acid-catabolizing enzymes described to contribute to MDSC-mediated T cell suppression in different settings, are potently inhibited by the commercially available chemical compounds L-NMMA, NOR-NOHA and 1-MDT, respectively [136-138]. Therefore *in vitro* suppression assays with *ex vivo* isolated, IAV-induced lung mono-MDSC in the presence or absence of these compounds were performed. Chemical inhibition of Arg1 and IDO had no effect on suppressive activity (Fig. 22). However, addition of the iNOS inhibitor completely blocked suppressive activity by IAV-induced lung mono-MDSC (Fig. 22). Hence, iNOS activity is the key mechanism applied by mono-MDSC from lungs of IAV-infected mice to suppress T cell proliferation. Taken together, the data show that mono-MDSC accumulate in the lungs of IAV-infected mice in the beginning of the adaptive response, suppressing T cell proliferation via iNOS expression.

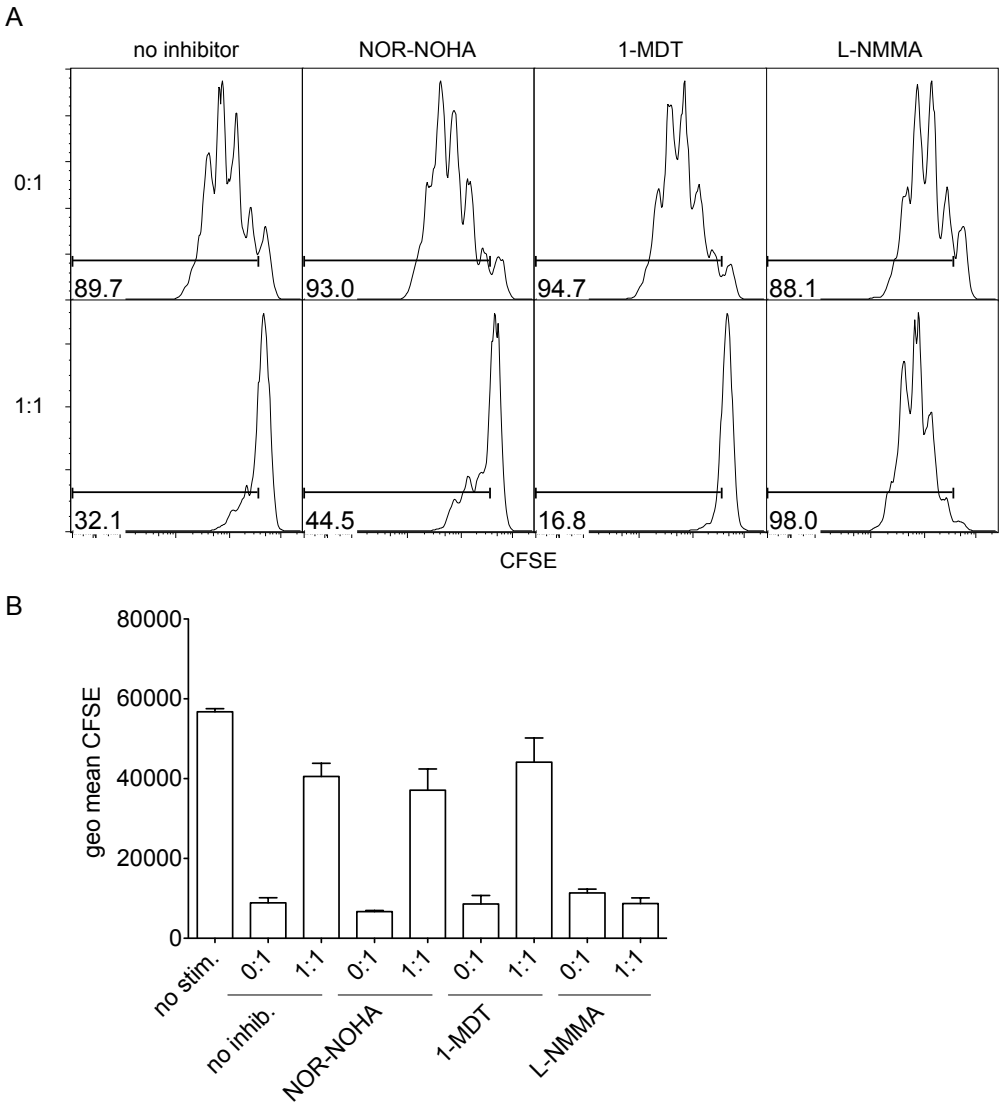

Figure 22: T cell suppression by IAV-induced lung mono-MDSC is iNOS-dependent.
A: histograms show dilution of CFSE in Tnaïves pre-gated and incubated as in Figure 17 but in presence or absence of NOR-NOHA, 1-MDT or L-NMMA (inhibitors of arginase, IDO and NOS, respectively). Numbers are frequencies of T cells undergoing at least one division. Each condition was performed in triplicates and representative data are shown. Data from one out of two independent experiments with comparable results are shown. *B*: geometric mean fluorescence intensity (geo mean) of CFSE in Tnaïves from the same experiment as in *A* is shown. Error bars show standard deviation.

In summary, the results reported in the second part of this thesis provide evidence that IAV induces accumulation of mono-MDSC with the ability to suppress T cell proliferation. These observations shed new light on the role of lung-infiltrating monocytes, which have long been considered to enhance

inflammation during IAV infection. The data indicate that at least part of the infiltrating monocytes are not fully differentiated TiP-DC and have the ability to inhibit a T cell response by means of iNOS expression, a hallmark of MDSC.

7. Discussion

The results from the first part of this study presented indications that the mechanisms contributing to Treg homeostasis in LN and spleen quantitatively differ. This was supported by a combined *in vivo* and *in silico* approach, for which the first multi-organ mathematical model of Treg homeostasis in mice was built. Additionally, using an *in vivo* Treg depletion strategy, Treg-mediated immune homeostasis was described to act in a broad immunological context, affecting a range of immune cell subsets such as B cells, NK cells and myeloid cells. Here again, fundamental differences in the responses in LN and spleen were observed. These findings might be of relevance since Treg depletion is currently considered a potential strategy for boosting vaccination and immunotherapies, making it essential to understand how the immune system reacts as a whole to such an intervention. The second part of this work focused on the role of MDSC in IAV infection and the results contributed evidence that mono-MDSC, which are able to suppress T cells, accumulate after acute respiratory infection with IAV. Since monocytes are considered to induce strong inflammation upon infiltration into IAV-infected lungs, these observations expand the knowledge on the role of monocytes during IAV infection. These findings should lead to a reconsideration of the role of monocytes in IAV infection as well as lead the way to further studies on the development of MDSC in acute infections.

7.1. Tregs and their role in keeping immune homeostasis in secondary lymphoid organs

7.1.1. Mechanisms of Treg homeostasis quantitatively differ in LN and spleen

T cell populations were observed to differ in LN and spleen in homeostatic state. The ratio of Tregs to Tnaïves is higher in the spleen, and the percentage of $CD69^+$ Tnaïves and Tregs is higher in LN. This was considered to be in agreement with the magnitude of antigen presentation, which is assumed to be lower in spleen, where adaptive immunity is initiated in case of blood-borne pathogen infection, and higher in peripheral LN, which

permanently survey a plethora of skin commensals and potentially pathogenic agents [42; 139]. Beside the differences observed in homeostatic state, it was also found here that Tnaïve dynamics fundamentally differ in LN and spleen following *in vivo* Treg depletion. The spleen was characterized by a transient reduction of the total Tnaïve population, in sharp contrast to LN, where Tnaïves transiently accumulated. Interestingly, only by introducing the assumption that Tregs influence Tnaïve migration it was possible to reproduce these experimental data *in silico*. In addition to direct killing and inactivation of Tnaïves by Tregs as well as indirect suppression by competition for antigen-presenting cells and cytokines [120], these results may add a new layer of immune control by Tregs, namely modulation of T cell migration properties. Keeping in mind the efforts to modulate Treg activity in clinical settings [2; 3], further studies should consider relocation of Tnaïves between different organs as a side effect of treatment. Further, only a dynamic recirculation of Tnaïves between LN and spleen could describe the *in vivo* results, implicating that factors influencing Tnaïve motility sense changes in population size. Such a quorum sensing-like mechanism has been reported to control homeostasis of T cell numbers [140]. The results described here expand this notion by adding that quorum sensing might also regulate trans-organ migration. However, it cannot be excluded that more complicated mechanistic differences between the organs would also contribute to the structural differences in the reconstitution dynamics.

Tnaïves use similar pathways to pass through LN and spleen [139; 141]. Tnaïves in peripheral blood expressing CD62L and CCR7 interact with high endothelial venules (HEV) of LN, which eventually leads to transendothelial migration and LN entry. Similarly, Tnaïves flowing with the blood stream within the marginal sinus and marginal zone of the spleen use related molecular pathways to achieve the splenic white pulp [139; 141]. Exit of LN and spleen is regulated by sphingosine-1-phosphate sensing in both LN and spleen [139; 141]. One important difference between LN and spleen with regard to Tnaïve migration is the exclusive presence of HEV in LN [142]. Interestingly, DC were shown to control T cell entry to LN via modulation of HEV function and it was discussed whether DC can regulate not only

phenotype but also growth of HEV [142; 143]. Since DC homeostasis is maintained by Tregs [44; 45], Tregs might be at least indirectly involved in HEV homeostasis. There is evidence for this assumption coming from studies of tumor-bearing mice in which Treg depletion leads to increased HEV formation within tumors [144]. This was associated with higher T cell infiltration and enhanced tumor control. To test whether Treg depletion changes HEV phenotype and/or growth, it would be interesting to quantify the number of HEV in LN of DEREG mice after DT injection as well as to assess their expression of maturation markers. This could be achieved by immunohistochemical staining for CD31, MECA-79, GLYCAM1, FucT-VII, GlcNAc6ST-2 and MADCAM1, as mature HEV were described to have a MECA-79$^+$GLYCAM1$^+$FucT-VII$^+$GlcNAc6ST-2$^+$MADCAM1$^-$ phenotype [143]. In case Tregs indeed control HEV homeostasis not only in tumors but also in LN, this could have effects on lymphocyte migration specifically in LN but not in spleen, which in turn could explain some of the differences observed here with regard to differential accumulation of Tnaïves and other immune cell subsets in LN and spleen.

Interestingly, the measured steady state size of T cell subsets imposed to the mathematical model that Treg migration between organs is reduced at least 4-fold compared to Tnaïves. Furthermore, including Treg trans-organ migration into the fit routine resulted in a negligible amount of Treg migration. When imposing Treg trans-organ migration at 20 % of the migration rate of Tnaïves, a fit of comparable quality was generated but at the price of unrealistic resting state recirculation frequencies which are in contradiction with the known passage times of six to eight hours for Tnaïves in LN [124-126]. These data suggest that Tregs are more sessile than Tnaïves. This assumption is supported by the finding that the T cell receptor repertoire of Tregs but not of Tnaïves is clearly different in different LN [145]. However, the presence of Tregs in peripheral blood suggests that Treg indeed recirculate. Since Treg subsets were not considered in the model, it could be that the reduced Treg migration that was predicted here reflects the Treg compartment as a whole but does not hold necessarily true for each of the Treg subsets. It would be interesting to expand the model and include cTregs

and eTregs, for example, which have different migratory properties [33; 34]. In summary, the framework of the presented model predicts that Treg recirculation is reduced in comparison to Tnaïves, although the quantitative degree of Treg recirculation could not be identified and needs to be further investigated.

Depletion of 50 % of Tregs in mice was described before to induce an overshoot of Tregs in peripheral blood and spleen within some days, which was followed by a slow decrease to normal level after some weeks [121]. The results presented here also show that the Treg population reaches a size that is larger than the original homeostatic size upon both *in vivo* and *in silico* depletion and reconstitution. According to the model, this result depends on two important features. First, the rates of each mechanism contributing to the Treg population have to adapt to the Treg rebound with a delay. A fast depletion induces strongly changed target parameter values in all processes contributing to Treg reconstitution. The delay in adopting these target values induces the overshoot, because the populations also do not stop the reconstitution process instantly. Secondly, the model predicts that the overshoot only appears for strong depletions of 90 % and more (data not shown). For less strong depletions, reconstitution is slower, growing beyond the original homeostatic population size after two weeks in LN but not in spleen. This result does not reflect the data from 50 % depletion model described above [121], but is supported by another previous study in which depletion of Tregs by 70 % led to a rebound without overshoot in LN and spleen [127]. Independent of which percentage of Tregs depleted exactly leads to an overshoot of Tregs in mice and keeping in mind the potential of Treg depletion in the clinics mentioned before, it should be taken into consideration whether a too strong Treg depletion in clinical settings might induce a subsequent state of excessive tolerance due to a Treg overshoot. This could be actually rather prejudicial for cancer patients, for example, since Tregs are known to hamper a proper anti-tumor response.

IL-2 signals through its high affinity heterotrimeric receptor after binding to CD25 alone [123]. This leads to conformational changes in the IL-2 molecule,

which promotes binding of CD122 to IL-2, and the complex consisting of IL-2, CD25 and CD122 then binds to CD132. Phosphorylation of tyrosine residues in the CD122 tail then initiates a cascade pathway eventually leading to internalization and degradation of IL-2 [123]. On one hand, Tregs use this pathway to consume IL-2 from its environment and, on the other hand, IL-2 signaling is key to normal Treg homeostasis in peripheral organs [19; 20]. Surprisingly, CD122 is rapidly downregulated from the surface of Tregs upon DT treatment in DEREG mice. Since DT disrupts protein synthesis upon penetration into target cells [146], this result indicates a short half-life for CD122 in Tregs. It seems that a stable expression of this molecule on the Treg surface demands a continuous production of CD122 itself or of accessory proteins involved in CD122 transport to the cell surface. CD25 was not downregulated like CD122 in the Treg depletion experiments (data not shown), indicating that the different chains of the IL-2 receptor are differentially regulated. Indeed, among the IL-2 receptor chains, only CD25 is recycled to the cell surface upon IL-2-binding and internalization, whereas CD122 and CD132 are degraded [123]. Given its importance in Treg homeostasis, it would be intriguing to test whether the sensitivity of CD122 to protein synthesis-disrupting pathways is specific for Tregs or a broad regulatory mechanism present in other CD122-producing cells. Future studies could try to figure this out and, in case this phenomenon is Treg-specific, it could be explored in strategies aiming at disturbing Tregs *in vivo*.

The results presented here shed light on a fundamental part of Treg homeostasis, which is the extrathymic generation of Tregs. A basal level of conversion takes place in the steady state, which is in accordance with the hypothesis that peripheral homeostasis depends on presentation of self, food and flora-derived antigens under tolerogenic conditions, leading to conversion of Tnaïves into pTregs [25; 147]. Here again, an essential difference between LN and spleen was observed. In comparison, approximately three times more pTregs appear daily in LN. Although this was not considered as a quantitative prediction, it seems reasonable that Treg induction in LN takes place at higher rates than in spleen. Further, the contribution of conversion to Treg homeostasis in LN was predicted to be at least as important as thymic output

and homeostatic proliferation. This goes in line with the differences in the nature of antigen presentation in both organs, as LN are supposed to be a site prone to tolerance induction [148-150]. A recent study claimed that only migratory DC, which are hosted in LN but not in spleen, are able to induce conversion of Tnaïves into pTregs, restricting development and presence of converted Tregs to LN [151]. The results only partially reflect those findings, as a basal level of conversion in spleen was also found, which has also been reported by others [152]. Moreover, different groups have reported that different DC types from different organs favor tolerance via Treg induction [150; 153-156], so that it will be tempting to expand the model in order to predict what happens in other organs, such as the gastrointestinal tract, lung and liver, where peripheral Treg conversion and expansion plays an important role for maintenance of tolerance [157-160].

The detailed approach presented here, combining highly time-resolved experimental data with a mathematical model, gave new and important insights into Treg biology. Such quantitative approaches applied to studies of infection, organ transplantation or autoimmunity could pave the way to a more refined understanding of T cell homeostasis.

7.1.2. Broad context of immune regulation by Tregs and its underlying differences in LN and spleen

DC and NK cells showed a quite similar response to Treg ablation, accumulating rapidly in LN, which was maintained for around one week, but accumulating in spleen only after day six of DT injection, which lasted a shorter period of time. Tregs are known to control the size of both DC and NK cell populations [44; 45; 47-49], so that a direct effect of Treg depletion on DC and NK cells should be expected. However, the similar pattern of response observed might also be caused by a direct interaction between DC and NK cells, as described before. DC express the IL-15 receptor α chain, which is necessary for trans-presentation of IL-15, a survival and growth factor for mature NK cells in the periphery [161]. Accordingly, an increase in the number of DC should lead to an increase in IL-15 trans-presentation followed by an increase in the NK cell population. The Treg/DC/NK cell axis was

discussed before [162]. The authors showed that Tnaïve/DC interaction in the absence of Tregs led to enhanced IL-15 trans-presentation by DC *in vitro*, which in turn was claimed as mechanism contributing for NK cell accumulation in Treg-depleted secondary lymphoid organs [162]. Further investigations on the direct role of DC in controlling the NK cell population *in vivo* in the absence of Tregs could be performed, for example, by application of anti-IL-15 blocking antibody following Treg depletion in DEREG mice.

A surprising finding in this study was the appearance of mo-DC in Treg-depleted LN. As noted above, mo-DC are neither present in LN nor spleen in the steady state, but can be readily found in LN four days after DT treatment in DEREG mice. Their presence was tightly controlled in time. Mechanistically, it might be due to monocyte activation by danger signals as a consequence of massive Treg death [163]. Since the spleen is responsible for blood filtering and elimination of dying erythrocytes, its apparatus for clearance of dead cells is likely much more efficient than that in LN [139]. This would mean that Treg death in peripheral tissues and their draining LN might induce much stronger danger signals when compared to death signal in the blood and spleen, leading to monocyte activation exclusively in LN. To assess whether mo-DC accumulation is indeed only due to accumulation of dead cells in peripheral tissues and LN and is not Treg-specific, DT injection in mice with bone marrow chimerism giving rise to 90 % wildtype T cells and 10 % T cells expressing the DT receptor [164] would provide a clearer picture. Such control experiments should also allow for discriminating whether other effects observed here after Treg depletion are indeed due to a Treg-specific role rather than due to a role of accumulation of dead cells. Independent of its mechanistic cause, induction of mo-DC in LN might be of special relevance considering the efforts for the development of strategies for vaccination boosting based on Treg depletion. mo-DC were described to express CCR7 as well as co-stimulatory molecules, such as CD40, CD80 and CD86, making them able to migrate to LN and potently present antigens in the context of both MHCI and MHCII [165]. It would be intriguing to test whether mo-DC accumulating in LN four days after Treg depletion can be used as targets for improving antigen presentation with the aim of boosting vaccination.

B cells are lymphocytes with the ability to produce antibodies. B cell development takes place in the bone marrow, where newly generated B cell receptors recognizing self-antigens are deleted from the repertoire. B cell deletion is one mechanism to prevent B cell recognition of own antigens. In secondary lymphoid organs, mature B cells, upon antigen recognition, interact with their cognate T cells, become activated, proliferate and secrete antibodies. Since the T cell repertoire is also selected not to react to self-antigens, T cell-mediated help of B cells is another mechanism for avoidance of a mistaken B cell response. Here it was found that B cells heavily accumulated in LN missing Tregs, which did not happen in the spleen. This observation makes it tempting to speculate on whether Tregs mediate B cell tolerance, which has been suggested before [50-52; 129]. Since activated Tnaïves, which can give rise to Tfh cells, accumulated alongside B cells in LN, it could be that Tregs indirectly control B cell homeostasis via modulation of Tfh cells. An argument against a role for Tregs in directly or indirectly controlling B cells is the fact that no overt signs of autoimmunity were observed in Treg-depleted mice even when they were kept for two months after treatment, although the very fast rebound of Tregs could have stopped B cells from developing a full response. Another explanation for the increased number of B cells in LN is that Tregs might control migration rather than activation/proliferation of B cells in this organ. Naïve B cells use similar pathways as Tnaïves to enter and exit LN, with selectins and CCR7-dependent interaction with HEV leading to LN entrance [166]. Therefore, it could be that Treg control of B cell accumulation in LN depends on similar mechanisms as those discussed above for Tnaïves. Again, such mechanisms could also explain why, in general, different lymphocyte subsets were observed accumulating selectively in LN but not in spleen.

In the steady state, neutrophils and monocytes are characterized as $CD11b^{+}Ly6C^{+}Ly6G^{+}$ cells and $CD11b^{+}Ly6C^{++}Ly6G^{-}$ cells, respectively [167]. Under certain inflammatory conditions, especially those found in chronic disease, these markers are also expressed by PMN-MDSC and mono-MDSC, respectively. A transient increase in the populations of $CD11b^{+}Ly6C^{+}Ly6G^{+}$ and $CD11b^{+}Ly6C^{++}Ly6G^{-}$ cells was detected in both LN and spleen upon Treg

ablation. *In vivo* Treg ablation leads to a very rapid accumulation of dead Tregs, which have to be promptly removed. Professional phagocytic cells such as monocytes and neutrophils exert this cleaning function. Therefore, accumulation of $CD11b^{+}Ly6C^{+}Ly6G^{+}$ and $CD11b^{+}Ly6C^{++}Ly6G^{-}$ cells in LN and spleen might be reflecting a systemic response to massive cell death with an increase in phagocytic cells. Other transgenic mouse lines, in which depletion of immune cell subsets are allowed by targeted DT receptor expression, also show accumulation of phagocytic cells [168]. From another point of view, one could speculate that $CD11b^{+}Ly6C^{+}Ly6G^{+}$ and $CD11b^{+}Ly6C^{++}Ly6G^{-}$ cells might be MDSC taking over immune control in absence of Tregs. This could also explain the lack of autoimmunity in DT-treated adult DEREG mice [111]. Both assumptions might be true and examining the suppressive activity of $CD11b^{+}Ly6C^{+}Ly6G^{+}$ and $CD11b^{+}Ly6C^{++}Ly6G^{-}$ cells from Treg-depleted mice would help answering this question.

In conclusion, Tregs were shown to be involved in controlling the immune response in a wide manner. Although further studies will be necessary for answering mechanistic questions, taken together the data demonstrate that immune modulation might be differentially achieved in LN and spleen, which could reflect the anatomical organization and function of these organs. Understanding how this takes place might help the development of more efficient immunotherapies and vaccination strategies boosting immune responses against chronic infections and tumors.

7.2. Accumulation of mono-MDSC during IAV infection

Many factors are involved in immune regulation during IAV infection. An elegant work surprisingly showed that IL-10 production by virus recognizing-specific, effector T cells is crucial to avoid immune-mediated lung disease and death in IAV-infected mice [104]. Tregs also seem to be involved in the immune response to IAV, since an expansion of IAV-specific Tregs in the lungs of infected mice was reported [105]. Despite the many pathways of immune regulation during IAV infection, the virus can induce excessive lung inflammation. Lung infiltration by monocytes, for example, is considered

detrimental for IAV infected mice, as these cells differentiate *in situ* into TiP-DC and exert overwhelming pro-inflammatory functions [65; 107; 108]. In the present study, new evidence was described that lung-infiltrating monocytes might actually exert an anti-inflammatory function, since they were able to suppress a T cell response. One explanation for this discrepancy – namely, the previously unrecognized anti-inflammatory role of lung infiltrating monocytes in IAV infection – might come from the fact that by now it is still difficult to distinguish between the progeny of infiltrating monocytes by means of surface markers and to study their function with *in vitro* functional assays. In one of the studies cited above, the authors combined the markers CD11c, MHCII, CD11b and Gr1 to sort and compare different lung cell populations with regard to their ability to induce proliferation of TCR-transgenic $CD8^+$ T cells isolated from the spleen of naïve mice [65]. In the other study, $CD11b^+Ly6C^{++}$ cells from the bronchoalveolar lavage of infected mice were sorted and examined for their ability to induce IL-2 expression in cells from a TCR-transgenic $CD8^+$ T cell hybridoma [107]. In this study, lung $CD11b^+Ly6C^{++}Ly6G^-$ cells were evaluated for their ability to suppress proliferation of polyclonally activated, wildtype $CD4^+$ Tnaïves. Therefore, direct comparison of the studies is challenging. Indeed, monocytes might differentiate in the same infected lung into either TiP-DC or mono-MDSC only depending on the microenvironmental milieu they are exposed to. Future work on additional differentiation markers and standardized functional assays are needed to shed light on the progeny of lung-infiltrating monocytes in IAV infection. A promising approach might involve transcriptome-based network analysis, which was used recently for, among others, a systematic phenotypic and functional characterization of human monocyte-derived macrophages upon activation [169].

IFNγ clearly plays a pleiotropic role in immune responses. Besides its pro-inflammatory activity, enhancing and/or inducing expression of MHCI and MHCII molecules and activating monocytes and macrophages, it can also promote isotype class-switch in B cells [170]. Interestingly, IFNγ can even dampen inflammation via, for example, induction of iNOS and IDO expression [171; 172]. In the present study, although blocking IFNγ *in vivo* led to a

significant decrease in the number of iNOS-producing cells in the lungs of IAV-infected mice, there was no difference in lung immunopathology as measured by changes in body weight and histology analysis. Furthermore, mono-MDSC from anti-IFNγ injected mice were able to suppress T cell proliferation *in vitro* as well as mono-MDSC from isotype control-injected mice. This was unexpected since previous work from our group with *in vivo* blockade showed that IFNγ has anti-inflammatory properties and plays a protective role in an antigen-specific, Th1-mediated skin inflammation model by inducing the local production of iNOS [132]. The discrepancy in the outcome of blocking IFNγ in immunopathology observed in these two models might arise from the inability of blocking IFNγ to completely stop iNOS expression in the IAV model – some $iNOS^+$ cells could still be found after treatment. It could also be that other, redundant regulatory mechanisms, such as enhanced Treg activity and production of IL-10 by infiltrating T cells, avoid lung damage during IAV infection in the absence of iNOS. Alternatively, the divergence might come from intrinsic differences in each model. The Th1-mediated skin inflammation model was induced by injection of antigen-specific, *in vitro* differentiated Th1 cells followed by subcutaneous application of the cognate antigen together with incomplete Freud adjuvant [132]. This model triggers a sterile inflammation of the skin. In contrast, the murine IAV infection model triggers a virus-mediated inflammation in the lungs. Therefore, both the nature of inflammation (sterile vs. non-sterile) as wells as its anatomical localization (skin vs. lung) might lead to different roles of IFNγ and/or different sensitivity of mono-MSDC to IFNγ. For a clearer picture of the role of IFNγ in this process, it could be informative to perform suppression assays with mono-MDSC isolated from the lungs of IAV-infected mice previously subjected to bone marrow chimerism using congenic-marked $IFN\gamma R^{+/+}$ and $IFN\gamma R^{-/-}$ cells. In case IFNγ is essential to switch on suppressive activity of IAV-induced mono-MDSC *in vivo*, $IFN\gamma R^{+/+}$ but not $IFN\gamma R^{-/-}$ mono-MDSC isolated from the same mice should prevent T cell proliferation *in vitro*. This could help elucidating the role of IFNγ as trigger of suppression by mono-MDSC. Additionally, in order to analyze whether mono-MDSC indeed prevent T cell proliferation *in vivo*, a reasonable experiment would be to stain

lung slides from IAV-infected mice immunohistochemically for CD3, Ki-67 and iNOS. $CD3^+$ T cells localizing close to iNOS producing cells should show no expression of Ki-67, which is a marker expressed in all mitotic phases of eukaryotic cells. In such an experiment, one could compare proliferation of T cells *in situ* in control mice and mice with blocked iNOS activity.

As discussed above, the strategy to block iNOS expression *in vivo* via injection of a blocking anti-IFNγ antibody did not lead to changes in lung immunopathology. Interestingly, iNOS chemical or genetic blockade improves resistance of mice to lethal IAV doses, which led to the conclusion that excessive iNOS and NO are actually toxic and promote rather than prevent lung immunopathology in the IAV-infected lung [173-175]. In those studies, it was discussed whether production of NO, a highly toxic reactive nitrogen species, leads to destruction of delicate lung tissues. Therefore, iNOS-producing mono-MDSC might not be essential for safeguarding lung tissues from T cell-induced immunopathology in IAV infection. However, mono-MDSC might play a role in formation of memory T cells. Following this line of thinking, iNOS expression by mono-MDSC might be responsible for avoiding massive proliferation of single clones of T cells infiltrating the lungs in the beginning of the T cell phase. This is also the period of time in which most mono-MDSC, IFNγ and iNOS are present in the infected lungs. Indeed, different groups claimed that IFNγ regulates memory T cell differentiation in T cell intrinsic but also extrinsic manners [176; 177]. More importantly, a recent report demonstrated that IFNγ acts limiting the memory T cell population size in IAV infection [178]. Therefore, it would be intriguing to test whether formation of memory T cell response is altered in IAV-infected mice in the absence of iNOS or mono-MDSC. This could unveil a new mechanism of regulation of memory T cells via the IFNγ/mono-MDSC/iNOS axis.

In summary, monocytes were shown here to infiltrate the lungs of IAV-infected mice and to develop into mono-MDSC, which show suppressive activity and hamper T cell proliferation *in vitro*. Therefore, this study provides evidence that MDSC can also appear during acute virus infection. Suppression activity was dependent on iNOS, the expression of which was

dependent on IFNγ *in vivo*. Although no enhanced lung immunopathology was observed upon IFNγ blockade *in vivo*, future studies might focus on the role of mono-MDSC in immunopathology under sterile/non-sterile conditions and in different organs as well as in regulating memory T cell response.

8. Conclusion and Outlook

This study helped shedding light on different aspects of the immune system, with a strong focus on immune regulation. First, fundamental differences in the response of LN and spleen Tregs and Tnaïves after Treg depletion were observed. A mathematical model based on temporal high resolution data of Treg depletion and reconstitution as well as of Tnaïve homeostasis predicted that Treg homeostasis mechanisms quantitatively differ in LN and spleen. Differences in LN and spleen immune cells were then demonstrated also in other subsets such as DC, NK cells and B cells. Although further mechanistic studies are needed for drawing more conclusions, it seems clear that Tregs are directly or indirectly involved in keeping immune homeostasis of a range of different cells. Finally, the ability of monocytes to differentiate into mono-MDSC upon IAV infection was evidenced, which led to suppression of a T cell response via iNOS production. This might lead to a reconsideration of the role of monocytes in this infection model and further studies might clarify the role of IFNγ/iNOS/mono-MDSC in regulating different types of inflammation in different organs and as well as in formation of memory T cells. Understanding immune regulation during IAV infection might lead to the ultimate goal of avoiding immune-mediated lung damage and associated death.

9. References

1 Sakaguchi, S. (2005). **Naturally arising Foxp3-expressing $CD25^+CD4^+$ regulatory T cells in immunological tolerance to self and non-self**. *Nat. Immunol.* 6, 345-352.

2 Webster, K.E., Walters, S., Kohler, R.E., Mrkvan, T., Boyman, O., Surh, C.D., Grey, S.T., and Sprent, J. (2009). **In vivo expansion of T reg cells with IL-2-mAb complexes: induction of resistance to EAE and long-term acceptance of islet allografts without immunosuppression**. *J. Exp. Med.* 206, 751-760.

3 Klages, K., Mayer, C.T., Lahl, K., Loddenkemper, C., Teng, M.W., Ngiow, S.F., Smyth, M.J., Hamann, A., Huehn, J., and Sparwasser, T. (2010). **Selective depletion of $Foxp3^+$ regulatory T cells improves effective therapeutic vaccination against established melanoma**. *Cancer Res.* 70, 7788-7799.

4 Hori, S., Nomura, T., and Sakaguchi, S. (2003). **Control of regulatory T cell development by the transcription factor Foxp3**. *Science* 299, 1057-1061.

5 Fontenot, J.D., Gavin, M.A., and Rudensky, A.Y. (2003). **Foxp3 programs the development and function of $CD4^+CD25^+$ regulatory T cells**. *Nat. Immunol.* 4, 330-336.

6 Khattri, R., Cox, T., Yasayko, S.A., and Ramsdell, F. (2003). **An essential role for Scurfin in $CD4^+CD25^+$ T regulatory cells**. *Nat. Immunol.* 4, 337-342.

7 Bennett, C.L., Christie, J., Ramsdell, F., Brunkow, M.E., Ferguson, P.J., Whitesell, L., Kelly, T.E., Saulsbury, F.T., Chance, P.F., and Ochs, H.D. (2001). **The immune dysregulation, polyendocrinopathy, enteropathy, X-linked syndrome (IPEX) is caused by mutations of FOXP3**. *Nat. Genet.* 27, 20-21.

8 Brunkow, M.E., Jeffery, E.W., Hjerrild, K.A., Paeper, B., Clark, L.B., Yasayko, S.A., Wilkinson, J.E., Galas, D., Ziegler, S.F., and Ramsdell, F. (2001). **Disruption of a new forkhead/winged-helix protein, scurfin, results in the fatal lymphoproliferative disorder of the scurfy mouse**. *Nat. Genet.* 27, 68-73.

9 Wildin, R.S., Ramsdell, F., Peake, J., Faravelli, F., Casanova, J.L., Buist, N., Levy-Lahad, E., Mazzella, M., Goulet, O., Perroni, L., Bricarelli, F.D., Byrne, G., McEuen, M., Proll, S., Appleby, M., and Brunkow, M.E. (2001). **X-linked neonatal diabetes mellitus, enteropathy and endocrinopathy syndrome is the human equivalent of mouse scurfy**. *Nat. Genet.* 27, 18-20.

10 Gavin, M.A., Rasmussen, J.P., Fontenot, J.D., Vasta, V., Manganiello, V.C., Beavo, J.A., and Rudensky, A.Y. (2007). **Foxp3-dependent programme of regulatory T-cell differentiation**. *Nature* 445, 771-775.

11 Lin, W., Haribhai, D., Relland, L.M., Truong, N., Carlson, M.R., Williams, C.B., and Chatila, T.A. (2007). **Regulatory T cell development in the absence of functional Foxp3**. *Nat. Immunol.* 8, 359-368.

12 Floess, S., Freyer, J., Siewert, C., Baron, U., Olek, S., Polansky, J., Schlawe, K., Chang, H.D., Bopp, T., Schmitt, E., Klein-Hessling, S., Serfling, E., Hamann, A., and Huehn, J. (2007). **Epigenetic control of the foxp3 locus in regulatory T cells**. *PLoS Biol.* 5, e38.

13 Polansky, J.K., Kretschmer, K., Freyer, J., Floess, S., Garbe, A., Baron, U., Olek, S., Hamann, A., von Boehmer, H., and Huehn, J. (2008). **DNA methylation controls Foxp3 gene expression**. *Eur. J. Immunol.* 38, 1654-1663.

14 Ohkura, N., Hamaguchi, M., Morikawa, H., Sugimura, K., Tanaka, A., Ito, Y., Osaki, M., Tanaka, Y., Yamashita, R., Nakano, N., Huehn, J., Fehling, H.J.,

Sparwasser, T., Nakai, K., and Sakaguchi, S. (2012). **T Cell Receptor Stimulation-Induced Epigenetic Changes and Foxp3 Expression Are Independent and Complementary Events Required for Treg Cell Development**. *Immunity* 10.1016/j.immuni.2012.09.010.

15 Toker, A., Engelbert, D., Garg, G., Polansky, J.K., Floess, S., Miyao, T., Baron, U., Duber, S., Geffers, R., Giehr, P., Schallenberg, S., Kretschmer, K., Olek, S., Walter, J., Weiss, S., Hori, S., Hamann, A., and Huehn, J. (2013). **Active Demethylation of the Foxp3 Locus Leads to the Generation of Stable Regulatory T Cells within the Thymus**. *J. Immunol.* 10.4049/jimmunol.1203473.

16 Wing, K., Onishi, Y., Prieto-Martin, P., Yamaguchi, T., Miyara, M., Fehervari, Z., Nomura, T., and Sakaguchi, S. (2008). **CTLA-4 control over Foxp3$^+$ regulatory T cell function**. *Science* 322, 271-275.

17 Qureshi, O.S., Zheng, Y., Nakamura, K., Attridge, K., Manzotti, C., Schmidt, E.M., Baker, J., Jeffery, L.E., Kaur, S., Briggs, Z., Hou, T.Z., Futter, C.E., Anderson, G., Walker, L.S., and Sansom, D.M. (2011). **Trans-endocytosis of CD80 and CD86: a molecular basis for the cell-extrinsic function of CTLA-4**. *Science* 332, 600-603.

18 Pandiyan, P., Zheng, L., Ishihara, S., Reed, J., and Lenardo, M.J. (2007). **CD4$^+$CD25$^+$Foxp3$^+$ regulatory T cells induce cytokine deprivation-mediated apoptosis of effector CD4$^+$ T cells**. *Nat. Immunol.* 8, 1353-1362.

19 Yu, A., Zhu, L., Altman, N.H., and Malek, T.R. (2009). **A low interleukin-2 receptor signaling threshold supports the development and homeostasis of T regulatory cells**. *Immunity* 30, 204-217.

20 Cheng, G., Yu, A., Dee, M.J., and Malek, T.R. (2013). **IL-2R signaling is essential for functional maturation of regulatory T cells during thymic development**. *J. Immunol.* 190, 1567-1575.

21 Schubert, L.A., Jeffery, E., Zhang, Y., Ramsdell, F., and Ziegler, S.F. (2001). **Scurfin (FOXP3) acts as a repressor of transcription and regulates T cell activation**. *J. Biol. Chem.* 276, 37672-37679.

22 Lio, C.W., and Hsieh, C.S. (2008). **A two-step process for thymic regulatory T cell development**. *Immunity* 28, 100-111.

23 Lathrop, S.K., Bloom, S.M., Rao, S.M., Nutsch, K., Lio, C.W., Santacruz, N., Peterson, D.A., Stappenbeck, T.S., and Hsieh, C.S. (2011). **Peripheral education of the immune system by colonic commensal microbiota**. *Nature* 478, 250-254.

24 Thorstenson, K.M., and Khoruts, A. (2001). **Generation of anergic and potentially immunoregulatory CD25$^+$CD4 T cells in vivo after induction of peripheral tolerance with intravenous or oral antigen**. *J. Immunol.* 167, 188-195.

25 Kretschmer, K., Apostolou, I., Hawiger, D., Khazaie, K., Nussenzweig, M.C., and von Boehmer, H. (2005). **Inducing and expanding regulatory T cell populations by foreign antigen**. *Nat. Immunol.* 12, 1219-1227.

26 Atarashi, K., Tanoue, T., Shima, T., Imaoka, A., Kuwahara, T., Momose, Y., Cheng, G., Yamasaki, S., Saito, T., Ohba, Y., Taniguchi, T., Takeda, K., Hori, S., Ivanov, II, Umesaki, Y., Itoh, K., and Honda, K. (2011). **Induction of colonic regulatory T cells by indigenous Clostridium species**. *Science* 331, 337-341.

27 Haribhai, D., Williams, J.B., Jia, S., Nickerson, D., Schmitt, E.G., Edwards, B., Ziegelbauer, J., Yassai, M., Li, S.H., Relland, L.M., Wise, P.M., Chen, A., Zheng, Y.Q., Simpson, P.M., Gorski, J., Salzman, N.H., Hessner, M.J., Chatila, T.A., and Williams, C.B. (2011). **A Requisite Role for Induced Regulatory T Cells in Tolerance Based on Expanding Antigen Receptor Diversity**. *Immunity* 35, 109-122.

28 Huang, Y.J., Haist, V., Baumgartner, W., Fohse, L., Prinz, I., Suerbaum, S., Floess, S., and Huehn, J. (2013). **Induced and thymus-derived Foxp3 regulatory T cells share a common niche**. *Eur. J. Immunol.* 10.1002/eji.201343463.

29 Thornton, A.M., Korty, P.E., Tran, D.Q., Wohlfert, E.A., Murray, P.E., Belkaid, Y., and Shevach, E.M. (2010). **Expression of Helios, an Ikaros transcription factor family member, differentiates thymic-derived from peripherally induced Foxp3$^+$ T regulatory cells**. *J. Immunol.* 184, 3433-3441.

30 Yadav, M., Louvet, C., Davini, D., Gardner, J.M., Martinez-Llordella, M., Bailey-Bucktrout, S., Anthony, B.A., Sverdrup, F.M., Head, R., Kuster, D.J., Ruminski, P., Weiss, D., Von Schack, D., and Bluestone, J.A. (2012). **Neuropilin-1 distinguishes natural and inducible regulatory T cells among regulatory T cell subsets in vivo**. *J. Exp. Med.* 209, 1713-1722.

31 Weiss, J.M., Bilate, A.M., Gobert, M., Ding, Y., Curotto de Lafaille, M.A., Parkhurst, C.N., Xiong, H., Dolpady, J., Frey, A.B., Ruocco, M.G., Yang, Y., Floess, S., Huehn, J., Oh, S., Li, M.O., Niec, R.E., Rudensky, A.Y., Dustin, M.L., Littman, D.R., and Lafaille, J.J. (2012). **Neuropilin 1 is expressed on thymus-derived natural regulatory T cells, but not mucosa-generated induced Foxp3$^+$ T reg cells**. *J. Exp. Med.* 10.1084/jem.20120914.

32 Akimova, T., Beier, U.H., Wang, L., Levine, M.H., and Hancock, W.W. (2011). **Helios expression is a marker of T cell activation and proliferation**. *PLoS One* 6, e24226.

33 Huehn, J., and Hamann, A. (2005). **Homing to suppress: address codes for Treg migration**. *Trends Immunol.* 26, 632-636.

34 Smigiel, K.S., Richards, E., Srivastava, S., Thomas, K.R., Dudda, J.C., Klonowski, K.D., and Campbell, D.J. (2014). **CCR7 provides localized access to IL-2 and defines homeostatically distinct regulatory T cell subsets**. *J. Exp. Med.* 211, 121-136.

35 Rubtsov, Y.P., Rasmussen, J.P., Chi, E.Y., Fontenot, J., Castelli, L., Ye, X., Treuting, P., Siewe, L., Roers, A., Henderson, W.R., Jr., Muller, W., and Rudensky, A.Y. (2008). **Regulatory T cell-derived interleukin-10 limits inflammation at environmental interfaces**. *Immunity* 28, 546-558.

36 Feuerer, M., Herrero, L., Cipolletta, D., Naaz, A., Wong, J., Nayer, A., Lee, J., Goldfine, A.B., Benoist, C., Shoelson, S., and Mathis, D. (2009). **Lean, but not obese, fat is enriched for a unique population of regulatory T cells that affect metabolic parameters**. *Nat. Med.* 15, 930-939.

37 Rosenblum, M.D., Gratz, I.K., Paw, J.S., Lee, K., Marshak-Rothstein, A., and Abbas, A.K. (2011). **Response to self antigen imprints regulatory memory in tissues**. *Nature* 480, 538-542.

38 Burzyn, D., Kuswanto, W., Kolodin, D., Shadrach, J.L., Cerletti, M., Jang, Y., Sefik, E., Tan, T.G., Wagers, A.J., Benoist, C., and Mathis, D. (2013). **A special population of regulatory T cells potentiates muscle repair**. *Cell* 155, 1282-1295.

39 Liston, A., and Gray, D.H. (2014). **Homeostatic control of regulatory T cell diversity**. *Nat. Rev. Immunol.* 10.1038/nri3605.

40 Koch, M.A., Tucker-Heard, G., Perdue, N.R., Killebrew, J.R., Urdahl, K.B., and Campbell, D.J. (2009). **The transcription factor T-bet controls regulatory T cell homeostasis and function during type 1 inflammation**. *Nat. Immunol.* 10, 595-602.

41 Chung, Y., Tanaka, S., Chu, F., Nurieva, R.I., Martinez, G.J., Rawal, S., Wang, Y.H., Lim, H., Reynolds, J.M., Zhou, X.H., Fan, H.M., Liu, Z.M., Neelapu, S.S., and Dong, C. (2011). **Follicular regulatory T cells expressing Foxp3 and Bcl-6 suppress germinal center reactions**. *Nat.*

Med. 17, 983-988.

42 Banchereau, J., Briere, F., Caux, C., Davoust, J., Lebecque, S., Liu, Y.J., Pulendran, B., and Palucka, K. (2000). **Immunobiology of dendritic cells**. *Annu. Rev. Immunol.* 18, 767-811.

43 Jenkins, M.K., Khoruts, A., Ingulli, E., Mueller, D.L., McSorley, S.J., Reinhardt, R.L., Itano, A., and Pape, K.A. (2001). **In vivo activation of antigen-specific CD4 T cells**. *Annu. Rev. Immunol.* 19, 23-45.

44 Darrasse-Jeze, G., Deroubaix, S., Mouquet, H., Victora, G.D., Eisenreich, T., Yao, K.H., Masilamani, R.F., Dustin, M.L., Rudensky, A., Liu, K., and Nussenzweig, M.C. (2009). **Feedback control of regulatory T cell homeostasis by dendritic cells in vivo**. *J. Exp. Med.* 206, 1853-1862.

45 Liu, K., Victora, G.D., Schwickert, T.A., Guermonprez, P., Meredith, M.M., Yao, K., Chu, F.F., Randolph, G.J., Rudensky, A.Y., and Nussenzweig, M. (2009). **In vivo analysis of dendritic cell development and homeostasis**. *Science* 324, 392-397.

46 Cooper, M.A., Fehniger, T.A., and Caligiuri, M.A. (2001). **The biology of human natural killer-cell subsets**. *Trends Immunol.* 22, 633-640.

47 Gasteiger, G., Hemmers, S., Bos, P.D., Sun, J.C., and Rudensky, A.Y. (2013). **IL-2-dependent adaptive control of NK cell homeostasis**. *J. Exp. Med.* 210, 1179-1187.

48 Gasteiger, G., Hemmers, S., Firth, M.A., Le Floc'h, A., Huse, M., Sun, J.C., and Rudensky, A.Y. (2013). **IL-2-dependent tuning of NK cell sensitivity for target cells is controlled by regulatory T cells**. *J. Exp. Med.* 210, 1167-1178.

49 Sitrin, J., Ring, A., Garcia, K.C., Benoist, C., and Mathis, D. (2013). **Regulatory T cells control NK cells in an insulitic lesion by depriving them of IL-2**. *J. Exp. Med.* 210, 1153-1165.

50 Ludwig-Portugall, I., Hamilton-Williams, E.E., Gottschalk, C., and Kurts, C. (2008). **Cutting edge: CD25$^+$ regulatory T cells prevent expansion and induce apoptosis of B cells specific for tissue autoantigens**. *J. Immunol.* 181, 4447-4451.

51 Ludwig-Portugall, I., Hamilton-Williams, E.E., Gotot, J., and Kurts, C. (2009). **CD25$^+$ T(reg) specifically suppress auto-Ab generation against pancreatic tissue autoantigens**. *Eur. J. Immunol.* 39, 225-233.

52 Leonardo, S.M., Josephson, J.A., Hartog, N.L., and Gauld, S.B. (2010). **Altered B cell development and anergy in the absence of Foxp3**. *J. Immunol.* 185, 2147-2156.

53 Riewaldt, J., Duber, S., Boernert, M., Krey, M., Dembinski, M., Weiss, S., Garbe, A.I., and Kretschmer, K. (2012). **Severe Developmental B Lymphopoietic Defects in Foxp3-Deficient Mice are Refractory to Adoptive Regulatory T Cell Therapy**. *Front. Immunol.* 3, 141.

54 Bronte, V., and Zanovello, P. (2005). **Regulation of immune responses by L-arginine metabolism**. *Nat. Rev. Immunol.* 5, 641-654.

55 Gabrilovich, D.I., and Nagaraj, S. (2009). **Myeloid-derived suppressor cells as regulators of the immune system**. *Nat. Rev. Immunol.* 9, 162-174.

56 Greten, T.F., Manns, M.P., and Korangy, F. (2011). **Myeloid derived suppressor cells in human diseases**. *Int. Immunopharmacol.* 11, 802-807.

57 Yona, S., Kim, K.W., Wolf, Y., Mildner, A., Varol, D., Breker, M., Strauss-Ayali, D., Viukov, S., Guilliams, M., Misharin, A., Hume, D.A., Perlman, H., Malissen, B., Zelzer, E., and Jung, S. (2013). **Fate mapping reveals origins and dynamics of monocytes and tissue macrophages under homeostasis**. *Immunity* 38, 79-91.

58 Carlin, L.M., Stamatiades, E.G., Auffray, C., Hanna, R.N., Glover, L., Vizcay-Barrena, G., Hedrick, C.C., Cook, H.T., Diebold, S., and Geissmann, F.

(2013). **Nr4a1-dependent Ly6C(low) monocytes monitor endothelial cells and orchestrate their disposal**. *Cell* 153, 362-375.

59 Robbins, C.S., Hilgendorf, I., Weber, G.F., Theurl, I., Iwamoto, Y., Figueiredo, J.L., Gorbatov, R., Sukhova, G.K., Gerhardt, L.M., Smyth, D., Zavitz, C.C., Shikatani, E.A., Parsons, M., van Rooijen, N., Lin, H.Y., Husain, M., Libby, P., Nahrendorf, M., Weissleder, R., and Swirski, F.K. (2013). **Local proliferation dominates lesional macrophage accumulation in atherosclerosis**. *Nat. Med.* 19, 1166-1172.

60 Zigmond, E., Varol, C., Farache, J., Elmaliah, E., Satpathy, A.T., Friedlander, G., Mack, M., Shpigel, N., Boneca, I.G., Murphy, K.M., Shakhar, G., Halpern, Z., and Jung, S. (2012). **Ly6C^{hi} monocytes in the inflamed colon give rise to proinflammatory effector cells and migratory antigen-presenting cells**. *Immunity* 37, 1076-1090.

61 Cortez-Retamozo, V., Etzrodt, M., Newton, A., Rauch, P.J., Chudnovskiy, A., Berger, C., Ryan, R.J., Iwamoto, Y., Marinelli, B., Gorbatov, R., Forghani, R., Novobrantseva, T.I., Koteliansky, V., Figueiredo, J.L., Chen, J.W., Anderson, D.G., Nahrendorf, M., Swirski, F.K., Weissleder, R., and Pittet, M.J. (2012). **Origins of tumor-associated macrophages and neutrophils**. *Proc. Natl. Acad. Sci. U. S. A.* 109, 2491-2496.

62 Zigmond, E., and Jung, S. (2013). **Intestinal macrophages: well educated exceptions from the rule**. *Trends Immunol.* 34, 162-168.

63 Serbina, N.V., and Pamer, E.G. (2006). **Monocyte emigration from bone marrow during bacterial infection requires signals mediated by chemokine receptor CCR2**. *Nat. Immunol.* 7, 311-317.

64 Serbina, N.V., Salazar-Mather, T.P., Biron, C.A., Kuziel, W.A., and Pamer, E.G. (2003). **TNF/iNOS-producing dendritic cells mediate innate immune defense against bacterial infection**. *Immunity* 19, 59-70.

65 Lin, K.L., Suzuki, Y., Nakano, H., Ramsburg, E., and Gunn, M.D. (2008). **CCR2^{+} monocyte-derived dendritic cells and exudate macrophages produce influenza-induced pulmonary immune pathology and mortality**. *J. Immunol.* 180, 2562-2572.

66 Youn, J.I., Nagaraj, S., Collazo, M., and Gabrilovich, D.I. (2008). **Subsets of myeloid-derived suppressor cells in tumor-bearing mice**. *J. Immunol.* 181, 5791-5802.

67 Sawanobori, Y., Ueha, S., Kurachi, M., Shimaoka, T., Talmadge, J.E., Abe, J., Shono, Y., Kitabatake, M., Kakimi, K., Mukaida, N., and Matsushima, K. (2008). **Chemokine-mediated rapid turnover of myeloid-derived suppressor cells in tumor-bearing mice**. *Blood* 111, 5457-5466.

68 Movahedi, K., Guilliams, M., Van den Bossche, J., Van den Bergh, R., Gysemans, C., Beschin, A., De Baetselier, P., and Van Ginderachter, J.A. (2008). **Identification of discrete tumor-induced myeloid-derived suppressor cell subpopulations with distinct T cell-suppressive activity**. *Blood* 111, 4233-4244.

69 Lesokhin, A.M., Hohl, T.M., Kitano, S., Cortez, C., Hirschhorn-Cymerman, D., Avogadri, F., Rizzuto, G.A., Lazarus, J.J., Pamer, E.G., Houghton, A.N., Merghoub, T., and Wolchok, J.D. (2012). **Monocytic CCR2^{+} myeloid-derived suppressor cells promote immune escape by limiting activated CD8 T-cell infiltration into the tumor microenvironment**. *Cancer Res.* 72, 876-886.

70 Shi, C., and Pamer, E.G. (2011). **Monocyte recruitment during infection and inflammation**. *Nat. Rev. Immunol.* 11, 762-774.

71 Youn, J.I., Kumar, V., Collazo, M., Nefedova, Y., Condamine, T., Cheng, P., Villagra, A., Antonia, S., McCaffrey, J.C., Fishman, M., Sarnaik, A., Horna, P., Sotomayor, E., and Gabrilovich, D.I. (2013). **Epigenetic silencing of**

retinoblastoma gene regulates pathologic differentiation of myeloid cells in cancer. *Nat. Immunol.* 14, 211-220.

72 Huang, B., Pan, P.Y., Li, Q., Sato, A.I., Levy, D.E., Bromberg, J., Divino, C.M., and Chen, S.H. (2006). **Gr-1$^+$CD115$^+$ immature myeloid suppressor cells mediate the development of tumor-induced T regulatory cells and T-cell anergy in tumor-bearing host**. *Cancer Res.* 66, 1123-1131.

73 Serafini, P., Mgebroff, S., Noonan, K., and Borrello, I. (2008). **Myeloid-derived suppressor cells promote cross-tolerance in B-cell lymphoma by expanding regulatory T cells**. *Cancer Res.* 68, 5439-5449.

74 Sinha, P., Clements, V.K., Bunt, S.K., Albelda, S.M., and Ostrand-Rosenberg, S. (2007). **Cross-talk between myeloid-derived suppressor cells and macrophages subverts tumor immunity toward a type 2 response**. *J. Immunol.* 179, 977-983.

75 Terabe, M., Matsui, S., Park, J.M., Mamura, M., Noben-Trauth, N., Donaldson, D.D., Chen, W., Wahl, S.M., Ledbetter, S., Pratt, B., Letterio, J.J., Paul, W.E., and Berzofsky, J.A. (2003). **Transforming growth factor-beta production and myeloid cells are an effector mechanism through which CD1d-restricted T cells block cytotoxic T lymphocyte-mediated tumor immunosurveillance: abrogation prevents tumor recurrence**. *J. Exp. Med.* 198, 1741-1752.

76 Nagaraj, S., Gupta, K., Pisarev, V., Kinarsky, L., Sherman, S., Kang, L., Herber, D.L., Schneck, J., and Gabrilovich, D.I. (2007). **Altered recognition of antigen is a mechanism of CD8$^+$ T cell tolerance in cancer**. *Nat. Med.* 13, 828-835.

77 Munn, D.H., Shafizadeh, E., Attwood, J.T., Bondarev, I., Pashine, A., and Mellor, A.L. (1999). **Inhibition of T cell proliferation by macrophage tryptophan catabolism**. *J. Exp. Med.* 189, 1363-1372.

78 Yu, J., Du, W., Yan, F., Wang, Y., Li, H., Cao, S., Yu, W., Shen, C., Liu, J., and Ren, X. (2013). **Myeloid-derived suppressor cells suppress antitumor immune responses through IDO expression and correlate with lymph node metastasis in patients with breast cancer**. *J. Immunol.* 190, 3783-3797.

79 Sander, L.E., Sackett, S.D., Dierssen, U., Beraza, N., Linke, R.P., Muller, M., Blander, J.M., Tacke, F., and Trautwein, C. (2010). **Hepatic acute-phase proteins control innate immune responses during infection by promoting myeloid-derived suppressor cell function**. *J. Exp. Med.* 207, 1453-1464.

80 Mencacci, A., Montagnoli, C., Bacci, A., Cenci, E., Pitzurra, L., Spreca, A., Kopf, M., Sharpe, A.H., and Romani, L. (2002). **CD80$^+$Gr-1$^+$ myeloid cells inhibit development of antifungal Th1 immunity in mice with candidiasis**. *J. Immunol.* 169, 3180-3190.

81 Norris, B.A., Uebelhoer, L.S., Nakaya, H.I., Price, A.A., Grakoui, A., and Pulendran, B. (2013). **Chronic but not acute virus infection induces sustained expansion of myeloid suppressor cell numbers that inhibit viral-specific T cell immunity**. *Immunity* 38, 309-321.

82 Qin, A., Cai, W., Pan, T., Wu, K., Yang, Q., Wang, N., Liu, Y., Yan, D., Hu, F., Guo, P., Chen, X., Chen, L., Zhang, H., Tang, X., and Zhou, J. (2013). **Expansion of monocytic myeloid-derived suppressor cells dampens T cell function in HIV-1-seropositive individuals**. *J. Virol.* 87, 1477-1490.

83 Fortin, C., Huang, X., and Yang, Y. (2012). **NK cell response to vaccinia virus is regulated by myeloid-derived suppressor cells**. *J. Immunol.* 189, 1843-1849.

84 Cheung, C.Y., Poon, L.L., Lau, A.S., Luk, W., Lau, Y.L., Shortridge, K.F., Gordon, S., Guan, Y., and Peiris, J.S. (2002). **Induction of proinflammatory**

cytokines in human macrophages by influenza A (H5N1) viruses: a mechanism for the unusual severity of human disease? *Lancet* 360, 1831-1837.

85 Kobasa, D., Takada, A., Shinya, K., Hatta, M., Halfmann, P., Theriault, S., Suzuki, H., Nishimura, H., Mitamura, K., Sugaya, N., Usui, T., Murata, T., Maeda, Y., Watanabe, S., Suresh, M., Suzuki, T., Suzuki, Y., Feldmann, H., and Kawaoka, Y. (2004). **Enhanced virulence of influenza A viruses with the haemagglutinin of the 1918 pandemic virus**. *Nature* 431, 703-707.

86 Arbeitsgemeinschaft-Influenza (2013). **Bericht zur Epidemiologie der Influenza in Deutschland Saison 2012/13** (Berlin: Robert Koch Institute).

87 Taubenberger, J.K., and Morens, D.M. (2006). **1918 Influenza: the mother of all pandemics**. *Emerg. Infect. Dis.* 12, 15-22.

88 Trifonov, V., Khiabanian, H., and Rabadan, R. (2009). **Geographic dependence, surveillance, and origins of the 2009 influenza A (H1N1) virus**. *N. Engl. J. Med.* 361, 115-119.

89 Lambert, L.C., and Fauci, A.S. (2010). **Influenza vaccines for the future**. *N. Engl. J. Med.* 363, 2036-2044.

90 Naffakh, N., Tomoiu, A., Rameix-Welti, M.A., and van der Werf, S. (2008). **Host restriction of avian influenza viruses at the level of the ribonucleoproteins**. *Annu. Rev. Microbiol.* 62, 403-424.

91 Subbarao, K., and Joseph, T. (2007). **Scientific barriers to developing vaccines against avian influenza viruses**. *Nat. Rev. Immunol.* 7, 267-278.

92 Lam, T.T., Wang, J., Shen, Y., Zhou, B., Duan, L., Cheung, C.L., Ma, C., Lycett, S.J., Leung, C.Y., Chen, X., Li, L., Hong, W., Chai, Y., Zhou, L., Liang, H., Ou, Z., Liu, Y., Farooqui, A., Kelvin, D.J., Poon, L.L., Smith, D.K., Pybus, O.G., Leung, G.M., Shu, Y., Webster, R.G., Webby, R.J., Peiris, J.S., Rambaut, A., Zhu, H., and Guan, Y. (2013). **The genesis and source of the H7N9 influenza viruses causing human infections in China**. *Nature* 502, 241-244.

93 Skehel, J.J., and Wiley, D.C. (2000). **Receptor binding and membrane fusion in virus entry: the influenza hemagglutinin**. *Annu. Rev. Biochem.* 69, 531-569.

94 Kim, J.H., Resende, R., Wennekes, T., Chen, H.M., Bance, N., Buchini, S., Watts, A.G., Pilling, P., Streltsov, V.A., Petric, M., Liggins, R., Barrett, S., McKimm-Breschkin, J.L., Niikura, M., and Withers, S.G. (2013). **Mechanism-based covalent neuraminidase inhibitors with broad-spectrum influenza antiviral activity**. *Science* 340, 71-75.

95 Morens, D.M., Taubenberger, J.K., and Fauci, A.S. (2010). **The 2009 H1N1 pandemic influenza virus: what next?** *mBio* 1.

96 Morens, D.M., Taubenberger, J.K., and Fauci, A.S. (2013). **Pandemic influenza viruses--hoping for the road not taken**. *N. Engl. J. Med.* 368, 2345-2348.

97 Mansfield, K.G. (2007). **Viral tropism and the pathogenesis of influenza in the Mammalian host**. *Am. J. Pathol.* 171, 1089-1092.

98 Tumpey, T.M., and Belser, J.A. (2009). **Resurrected pandemic influenza viruses**. *Annu. Rev. Microbiol.* 63, 79-98.

99 Ibricevic, A., Pekosz, A., Walter, M.J., Newby, C., Battaile, J.T., Brown, E.G., Holtzman, M.J., and Brody, S.L. (2006). **Influenza virus receptor specificity and cell tropism in mouse and human airway epithelial cells**. *J. Virol.* 80, 7469-7480.

100 Matsuoka, Y., Lamirande, E.W., and Subbarao, K. (2009). **The ferret model for influenza**. *Current protocols in microbiology* Chapter 15, Unit 15G 12.

101 Corti, D., and Lanzavecchia, A. (2013). **Broadly neutralizing antiviral antibodies**. *Annu. Rev. Immunol.* 31, 705-742.

102 Hillaire, M.L., Rimmelzwaan, G.F., and Kreijtz, J.H. (2013). **Clearance of influenza virus infections by T cells: risk of collateral damage?** *Curr. Opin. Virol.* 3, 430-437.

103 Doherty, P.C., Topham, D.J., Tripp, R.A., Cardin, R.D., Brooks, J.W., and Stevenson, P.G. (1997). **Effector CD4$^+$ and CD8$^+$ T-cell mechanisms in the control of respiratory virus infections**. *Immunol. Rev.* 159, 105-117.

104 Sun, J., Madan, R., Karp, C.L., and Braciale, T.J. (2009). **Effector T cells control lung inflammation during acute influenza virus infection by producing IL-10**. *Nat. Med.* 15, 277-284.

105 Betts, R.J., Prabhu, N., Ho, A.W., Lew, F.C., Hutchinson, P.E., Rotzschke, O., Macary, P.A., and Kemeny, D.M. (2012). **Influenza A virus infection results in a robust, antigen-responsive, and widely disseminated Foxp3$^+$ regulatory T cell response**. *J. Virol.* 86, 2817-2825.

106 Brincks, E.L., Roberts, A.D., Cookenham, T., Sell, S., Kohlmeier, J.E., Blackman, M.A., and Woodland, D.L. (2013). **Antigen-specific memory regulatory CD4$^+$Foxp3$^+$ T cells control memory responses to influenza virus infection**. *J. Immunol.* 190, 3438-3446.

107 Aldridge, J.R., Jr., Moseley, C.E., Boltz, D.A., Negovetich, N.J., Reynolds, C., Franks, J., Brown, S.A., Doherty, P.C., Webster, R.G., and Thomas, P.G. (2009). **TNF/iNOS-producing dendritic cells are the necessary evil of lethal influenza virus infection**. *Proc. Natl. Acad. Sci. U. S. A.* 106, 5306-5311.

108 Pamer, E.G. (2009). **Tipping the balance in favor of protective immunity during influenza virus infection**. *Proc. Natl. Acad. Sci. U. S. A.* 106, 4961-4962.

109 Wang, J., Li, F., Sun, R., Gao, X., Wei, H., Li, L.J., and Tian, Z. (2013). **Bacterial colonization dampens influenza-mediated acute lung injury via induction of M2 alveolar macrophages**. *Nat Commun* 4, 2106.

110 De Santo, C., Salio, M., Masri, S.H., Lee, L.Y., Dong, T., Speak, A.O., Porubsky, S., Booth, S., Veerapen, N., Besra, G.S., Grone, H.J., Platt, F.M., Zambon, M., and Cerundolo, V. (2008). **Invariant NKT cells reduce the immunosuppressive activity of influenza A virus-induced myeloid-derived suppressor cells in mice and humans**. *J. Clin. Invest.* 118, 4036-4048.

111 Lahl, K., Loddenkemper, C., Drouin, C., Freyer, J., Arnason, J., Eberl, G., Hamann, A., Wagner, H., Huehn, J., and Sparwasser, T. (2007). **Selective depletion of Foxp3$^+$ regulatory T cells induces a scurfy-like disease**. *J. Exp. Med.* 204, 57-63.

112 Kim, J.M., Rasmussen, J.P., and Rudensky, A.Y. (2007). **Regulatory T cells prevent catastrophic autoimmunity throughout the lifespan of mice**. *Nat. Immunol.* 8, 191-197.

113 Kerdiles, Y., Ugolini, S., and Vivier, E. (2013). **T cell regulation of natural killer cells**. *J. Exp. Med.* 210, 1065-1068.

114 Srivastava, B., Blazejewska, P., Hessmann, M., Bruder, D., Geffers, R., Mauel, S., Gruber, A.D., and Schughart, K. (2009). **Host genetic background strongly influences the response to influenza a virus infections**. *PLoS One* 4, e4857.

115 Kittel, B., Ruehl-Fehlert, C., Morawietz, G., Klapwijk, J., Elwell, M.R., Lenz, B., O'Sullivan, M.G., Roth, D.R., and Wadsworth, P.F. (2004). **Revised guides for organ sampling and trimming in rats and mice--Part 2. A joint publication of the RITA and NACAD groups**. *Exp. Toxicol. Pathol.* 55, 413-431.

116 Bode, J., Dutow, P., Sommer, K., Janik, K., Glage, S., Tummler, B., Munder, A., Laudeley, R., Sachse, K.W., and Klos, A. (2012). **A new role of the**

complement system: C3 provides protection in a mouse model of lung infection with intracellular Chlamydia psittaci. *PLoS One* 7, e50327.

117 Freitas, A.A., and Rocha, B. (1999). **Peripheral T cell survival**. *Curr. Opin. Immunol.* 11, 152-156.

118 Busse, D., de la Rosa, M., Hobiger, K., Thurley, K., Flossdorf, M., Scheffold, A., and Hofer, T. (2010). **Competing feedback loops shape IL-2 signaling between helper and regulatory T lymphocytes in cellular microenvironments**. *Proc. Natl. Acad. Sci. U. S. A.* 107, 3058-3063.

119 Hofer, T., Krichevsky, O., and Altan-Bonnet, G. (2012). **Competition for IL-2 between Regulatory and Effector T Cells to Chisel Immune Responses**. *Front. Immunol.* 3, 268.

120 Sakaguchi, S., Yamaguchi, T., Nomura, T., and Ono, M. (2008). **Regulatory T cells and immune tolerance**. *Cell* 133, 775-787.

121 Pierson, W., Cauwe, B., Policheni, A., Schlenner, S.M., Franckaert, D., Berges, J., Humblet-Baron, S., Schonefeldt, S., Herold, M.J., Hildeman, D., Strasser, A., Bouillet, P., Lu, L.F., Matthys, P., Freitas, A.A., Luther, R.J., Weaver, C.T., Dooley, J., Gray, D.H., and Liston, A. (2013). **Antiapoptotic Mcl-1 is critical for the survival and niche-filling capacity of Foxp3$^+$ regulatory T cells**. *Nat. Immunol.* 14, 959-965.

122 Amado, I.F., Berges, J., Luther, R.J., Mailhe, M.P., Garcia, S., Bandeira, A., Weaver, C., Liston, A., and Freitas, A.A. (2013). **IL-2 coordinates IL-2-producing and regulatory T cell interplay**. *J. Exp. Med.* 210, 2707-2720.

123 Malek, T.R., and Castro, I. (2010). **Interleukin-2 receptor signaling: at the interface between tolerance and immunity**. *Immunity* 33, 153-165.

124 Pellas, T.C., and Weiss, L. (1990). **Migration pathways of recirculating murine B cells and CD4$^+$ and CD8$^+$ T lymphocytes**. *Am. J. Anat* 187, 355-373.

125 Young, A.J. (1999). **The physiology of lymphocyte migration through the single lymph node in vivo**. *Semin. Immunol.* 11, 73-83.

126 Tomura, M., Yoshida, N., Tanaka, J., Karasawa, S., Miwa, Y., Miyawaki, A., and Kanagawa, O. (2008). **Monitoring cellular movement in vivo with photoconvertible fluorescence protein "Kaede" transgenic mice**. *Proc. Natl. Acad. Sci. U. S. A.* 105, 10871-10876.

127 Suffner, J., Hochweller, K., Kuhnle, M.C., Li, X., Kroczek, R.A., Garbi, N., and Hammerling, G.J. (2010). **Dendritic cells support homeostatic expansion of Foxp3$^+$ regulatory T cells in Foxp3.LuciDTR mice**. *J. Immunol.* 184, 1810-1820.

128 Belz, G.T., and Nutt, S.L. (2012). **Transcriptional programming of the dendritic cell network**. *Nat. Rev. Immunol.* 12, 101-113.

129 Seo, S.J., Fields, M.L., Buckler, J.L., Reed, A.J., Mandik-Nayak, L., Nish, S.A., Noelle, R.J., Turka, L.A., Finkelman, F.D., Caton, A.J., and Erikson, J. (2002). **The impact of T helper and T regulatory cells on the regulation of anti-double-stranded DNA B cells**. *Immunity* 16, 535-546.

130 Bender, B.S., Croghan, T., Zhang, L., and Small, P.A., Jr. (1992). **Transgenic mice lacking class I major histocompatibility complex-restricted T cells have delayed viral clearance and increased mortality after influenza virus challenge**. *J. Exp. Med.* 175, 1143-1145.

131 Yap, K.L., and Ada, G.L. (1978). **Cytotoxic T cells in the lungs of mice infected with an influenza A virus**. *Scand. J. Immunol.* 7, 73-80.

132 Feuerer, M., Eulenburg, K., Loddenkemper, C., Hamann, A., and Huehn, J. (2006). **Self-limitation of Th1-mediated inflammation by IFN-gamma**. *J. Immunol.* 176, 2857-2863.

133 Nathan, C., and Shiloh, M.U. (2000). **Reactive oxygen and nitrogen intermediates in the relationship between mammalian hosts and**

microbial pathogens. *Proc. Natl. Acad. Sci. U. S. A.* 97, 8841-8848.

134 Sun, K., and Metzger, D.W. (2008). **Inhibition of pulmonary antibacterial defense by interferon-gamma during recovery from influenza infection**. *Nat. Med.* 14, 558-564.

135 Cottey, R., Rowe, C.A., and Bender, B.S. (2001). **Influenza virus**. *Curr. Protoc. Immunol.* Chapter 19, Unit 19 11.

136 Griffith, O.W., and Kilbourn, R.G. (1996). **Nitric oxide synthase inhibitors: amino acids**. *Methods Enzymol.* 268, 375-392.

137 Tenu, J.P., Lepoivre, M., Moali, C., Brollo, M., Mansuy, D., and Boucher, J.L. (1999). **Effects of the new arginase inhibitor N(omega)-hydroxy-nor-L-arginine on NO synthase activity in murine macrophages**. *Nitric Oxide* 3, 427-438.

138 Hou, D.Y., Muller, A.J., Sharma, M.D., DuHadaway, J., Banerjee, T., Johnson, M., Mellor, A.L., Prendergast, G.C., and Munn, D.H. (2007). **Inhibition of indoleamine 2,3-dioxygenase in dendritic cells by stereoisomers of 1-methyl-tryptophan correlates with antitumor responses**. *Cancer Res.* 67, 792-801.

139 Mebius, R.E., and Kraal, G. (2005). **Structure and function of the spleen**. *Nat. Rev. Immunol.* 5, 606-616.

140 Almeida, A.R., Amado, I.F., Reynolds, J., Berges, J., Lythe, G., Molina-Paris, C., and Freitas, A.A. (2012). **Quorum-Sensing in CD4$^+$ T Cell Homeostasis: A Hypothesis and a Model**. *Front. Immunol.* 3, 125.

141 Cyster, J.G., and Schwab, S.R. (2012). **Sphingosine-1-phosphate and lymphocyte egress from lymphoid organs**. *Annu. Rev. Immunol.* 30, 69-94.

142 Girard, J.P., Moussion, C., and Forster, R. (2012). **HEVs, lymphatics and homeostatic immune cell trafficking in lymph nodes**. *Nat. Rev. Immunol.* 12, 762-773.

143 Moussion, C., and Girard, J.P. (2011). **Dendritic cells control lymphocyte entry to lymph nodes through high endothelial venules**. *Nature* 479, 542-546.

144 Hindley, J.P., Jones, E., Smart, K., Bridgeman, H., Lauder, S.N., Ondondo, B., Cutting, S., Ladell, K., Wynn, K.K., Withers, D., Price, D.A., Ager, A., Godkin, A.J., and Gallimore, A.M. (2012). **T-cell trafficking facilitated by high endothelial venules is required for tumor control after regulatory T-cell depletion**. *Cancer Res.* 72, 5473-5482.

145 Lathrop, S.K., Santacruz, N.A., Pham, D., Luo, J., and Hsieh, C.S. (2008). **Antigen-specific peripheral shaping of the natural regulatory T cell population**. *J. Exp. Med.* 205, 3105-3117.

146 Hadfield, T.L., McEvoy, P., Polotsky, Y., Tzinserling, V.A., and Yakovlev, A.A. (2000). **The pathology of diphtheria**. *J. Infect. Dis.* 181 Suppl 1, S116-120.

147 Steinman, R.M., and Nussenzweig, M.C. (2002). **Avoiding horror autotoxicus: the importance of dendritic cells in peripheral T cell tolerance**. *Proc. Natl. Acad. Sci. U. S. A.* 99, 351-358.

148 Azukizawa, H., Dohler, A., Kanazawa, N., Nayak, A., Lipp, M., Malissen, B., Autenrieth, I., Katayama, I., Riemann, M., Weih, F., Berberich-Siebelt, F., and Lutz, M.B. (2011). **Steady state migratory RelB$^+$ langerin$^+$ dermal dendritic cells mediate peripheral induction of antigen-specific CD4$^+$ CD25$^+$ Foxp3$^+$ regulatory T cells**. *Eur. J. Immunol.* 41, 1420-1434.

149 Gomez de Aguero, M., Vocanson, M., Hacini-Rachinel, F., Taillardet, M., Sparwasser, T., Kissenpfennig, A., Malissen, B., Kaiserlian, D., and Dubois, B. (2012). **Langerhans cells protect from allergic contact dermatitis in mice by tolerizing CD8$^+$ T cells and activating Foxp3$^+$ regulatory T cells**. *J. Clin. Invest.* 122, 1700-1711.

150 Guilliams, M., Crozat, K., Henri, S., Tamoutounour, S., Grenot, P., Devilard, E., de Bovis, B., Alexopoulou, L., Dalod, M., and Malissen, B. (2010). **Skin-draining lymph nodes contain dermis-derived CD103- dendritic cells that constitutively produce retinoic acid and induce Foxp3$^+$ regulatory T cells**. *Blood* 115, 1958-1968.

151 Vitali, C., Mingozzi, F., Broggi, A., Barresi, S., Zolezzi, F., Bayry, J., Raimondi, G., Zanoni, I., and Granucci, F. (2012). **Migratory, and not lymphoid-resident, dendritic cells maintain peripheral self-tolerance and prevent autoimmunity via induction of iTreg cells**. *Blood* 120, 1237-1245.

152 Yamazaki, S., Dudziak, D., Heidkamp, G.F., Fiorese, C., Bonito, A.J., Inaba, K., Nussenzweig, M.C., and Steinman, R.M. (2008). **CD8$^+$ CD205$^+$ splenic dendritic cells are specialized to induce Foxp3$^+$ regulatory T cells**. *J. Immunol.* 181, 6923-6933.

153 Yamazaki, S., Bonito, A.J., Spisek, R., Dhodapkar, M., Inaba, K., and Steinman, R.M. (2007). **Dendritic cells are specialized accessory cells along with TGF- for the differentiation of Foxp3$^+$ CD4$^+$ regulatory T cells from peripheral Foxp3 precursors**. *Blood* 110, 4293-4302.

154 Coombes, J.L., Siddiqui, K.R., Arancibia-Carcamo, C.V., Hall, J., Sun, C.M., Belkaid, Y., and Powrie, F. (2007). **A functionally specialized population of mucosal CD103$^+$ DCs induces Foxp3$^+$ regulatory T cells via a TGF-beta and retinoic acid-dependent mechanism**. *J. Exp. Med.* 204, 1757-1764.

155 Sun, C.M., Hall, J.A., Blank, R.B., Bouladoux, N., Oukka, M., Mora, J.R., and Belkaid, Y. (2007). **Small intestine lamina propria dendritic cells promote de novo generation of Foxp3 Treg cells via retinoic acid**. *J. Exp. Med.* 204, 1775-1785.

156 van der Aar, A.M., Picavet, D.I., Muller, F.J., de Boer, L., van Capel, T.M., Zaat, S.A., Bos, J.D., Janssen, H., George, T.C., Kapsenberg, M.L., van Ham, S.M., Teunissen, M.B., and de Jong, E.C. (2013). **Langerhans cells favor skin flora tolerance through limited presentation of bacterial antigens and induction of regulatory T cells**. *J. Invest. Dermatol.* 133, 1240-1249.

157 Josefowicz, S.Z., Niec, R.E., Kim, H.Y., Treuting, P., Chinen, T., Zheng, Y., Umetsu, D.T., and Rudensky, A.Y. (2012). **Extrathymically generated regulatory T cells control mucosal TH2 inflammation**. *Nature* 482, 395-399.

158 Hadis, U., Wahl, B., Schulz, O., Hardtke-Wolenski, M., Schippers, A., Wagner, N., Muller, W., Sparwasser, T., Forster, R., and Pabst, O. (2011). **Intestinal tolerance requires gut homing and expansion of FoxP3$^+$ regulatory T cells in the lamina propria**. *Immunity* 34, 237-246.

159 Siewert, C., Lauer, U., Cording, S., Bopp, T., Schmitt, E., Hamann, A., and Huehn, J. (2008). **Experience-driven development: effector/memory-like alphaE$^+$Foxp3$^+$ regulatory T cells originate from both naive T cells and naturally occurring naive-like regulatory T cells**. *J. Immunol.* 180, 146-155.

160 Cording, S., Wahl, B., Kulkarni, D., Chopra, H., Pezoldt, J., Buettner, M., Dummer, A., Hadis, U., Heimesaat, M., Bereswill, S., Falk, C., Bode, U., Hamann, A., Fleissner, D., Huehn, J., and Pabst, O. (2013). **The intestinal micro-environment imprints stromal cells to promote efficient Treg induction in gut-draining lymph nodes**. *Mucosal Immunol.* 10.1038/mi.2013.54.

161 Marcais, A., Viel, S., Grau, M., Henry, T., Marvel, J., and Walzer, T. (2013). **Regulation of Mouse NK Cell Development and Function by Cytokines**. *Front. Immunol.* 4, 450.

162 Terme, M., Chaput, N., Combadiere, B., Ma, A., Ohteki, T., and Zitvogel, L.

(2008). **Regulatory T cells control dendritic cell/NK cell cross-talk in lymph nodes at the steady state by inhibiting CD4$^+$ self-reactive T cells**. *J. Immunol.* 180, 4679-4686.

163 Peter, C., Wesselborg, S., Herrmann, M., and Lauber, K. (2010). **Dangerous attraction: phagocyte recruitment and danger signals of apoptotic and necrotic cells**. *Apoptosis* 15, 1007-1028.

164 Buch, T., Heppner, F.L., Tertilt, C., Heinen, T.J., Kremer, M., Wunderlich, F.T., Jung, S., and Waisman, A. (2005). **A Cre-inducible diphtheria toxin receptor mediates cell lineage ablation after toxin administration**. *Nature methods* 2, 419-426.

165 Cheong, C., Matos, I., Choi, J.H., Dandamudi, D.B., Shrestha, E., Longhi, M.P., Jeffrey, K.L., Anthony, R.M., Kluger, C., Nchinda, G., Koh, H., Rodriguez, A., Idoyaga, J., Pack, M., Velinzon, K., Park, C.G., and Steinman, R.M. (2010). **Microbial stimulation fully differentiates monocytes to DC-SIGN/CD209$^+$ dendritic cells for immune T cell areas**. *Cell* 143, 416-429.

166 Park, C., Hwang, I.Y., Sinha, R.K., Kamenyeva, O., Davis, M.D., and Kehrl, J.H. (2012). **Lymph node B lymphocyte trafficking is constrained by anatomy and highly dependent upon chemoattractant desensitization**. *Blood* 119, 978-989.

167 Rose, S., Misharin, A., and Perlman, H. (2012). **A novel Ly6C/Ly6G-based strategy to analyze the mouse splenic myeloid compartment**. *Cytometry A* 81, 343-350.

168 Tittel, A.P., Heuser, C., Ohliger, C., Llanto, C., Yona, S., Hammerling, G.J., Engel, D.R., Garbi, N., and Kurts, C. (2012). **Functionally relevant neutrophilia in CD11c diphtheria toxin receptor transgenic mice**. *Nature methods* 9, 385-390.

169 Xue, J., Schmidt, S.V., Sander, J., Draffehn, A., Krebs, W., Quester, I., De Nardo, D., Gohel, T.D., Emde, M., Schmidleithner, L., Ganesan, H., Nino-Castro, A., Mallmann, M.R., Labzin, L., Theis, H., Kraut, M., Beyer, M., Latz, E., Freeman, T.C., Ulas, T., and Schultze, J.L. (2014). **Transcriptome-based network analysis reveals a spectrum model of human macrophage activation**. *Immunity* 40, 274-288.

170 Farrar, M.A., and Schreiber, R.D. (1993). **The molecular cell biology of interferon-gamma and its receptor**. *Annu. Rev. Immunol.* 11, 571-611.

171 Guillonneau, C., Hill, M., Hubert, F.X., Chiffoleau, E., Herve, C., Li, X.L., Heslan, M., Usal, C., Tesson, L., Menoret, S., Saoudi, A., Le Mauff, B., Josien, R., Cuturi, M.C., and Anegon, I. (2007). **CD40Ig treatment results in allograft acceptance mediated by CD8CD45RC T cells, IFN-gamma, and indoleamine 2,3-dioxygenase**. *J. Clin. Invest.* 117, 1096-1106.

172 Koblish, H.K., Hunter, C.A., Wysocka, M., Trinchieri, G., and Lee, W.M. (1998). **Immune suppression by recombinant interleukin (rIL)-12 involves interferon gamma induction of nitric oxide synthase 2 (iNOS) activity: inhibitors of NO generation reveal the extent of rIL-12 vaccine adjuvant effect**. *J. Exp. Med.* 188, 1603-1610.

173 Akaike, T., Noguchi, Y., Ijiri, S., Setoguchi, K., Suga, M., Zheng, Y.M., Dietzschold, B., and Maeda, H. (1996). **Pathogenesis of influenza virus-induced pneumonia: involvement of both nitric oxide and oxygen radicals**. *Proc. Natl. Acad. Sci. U. S. A.* 93, 2448-2453.

174 Karupiah, G., Chen, J.H., Mahalingam, S., Nathan, C.F., and MacMicking, J.D. (1998). **Rapid interferon gamma-dependent clearance of influenza A virus and protection from consolidating pneumonitis in nitric oxide synthase 2-deficient mice**. *J. Exp. Med.* 188, 1541-1546.

175 Perrone, L.A., Belser, J.A., Wadford, D.A., Katz, J.M., and Tumpey, T.M. (2013). **Inducible nitric oxide contributes to viral pathogenesis following**

highly pathogenic influenza virus infection in mice. *J. Infect. Dis.* 207, 1576-1584.

176 Sercan, O., Stoycheva, D., Hammerling, G.J., Arnold, B., and Schuler, T. (2010). **IFN-gamma receptor signaling regulates memory CD8$^+$ T cell differentiation**. *J. Immunol.* 184, 2855-2862.

177 Turner, S.J., Olivas, E., Gutierrez, A., Diaz, G., and Doherty, P.C. (2007). **Disregulated influenza A virus-specific CD8$^+$ T cell homeostasis in the absence of IFN-gamma signaling**. *J. Immunol.* 178, 7616-7622.

178 Prabhu, N., Ho, A.W., Wong, K.H., Hutchinson, P.E., Chua, Y.L., Kandasamy, M., Lee, D.C., Sivasankar, B., and Kemeny, D.M. (2013). **Gamma interferon regulates contraction of the influenza virus-specific CD8 T cell response and limits the size of the memory population**. *J. Virol.* 87, 12510-12522.

Acknowledgments

First I would like to thank my supervisor, Prof. Dr. Jochen Huehn, for the opportunity to work in his lab (and for the many hours in the lab being compensated by the many hours playing Kicker). Thank you, Jochen! Thanks also to the HZI GradSchool, DOIT and my co-supervisors, especially Prof. Dr. Michael Meyer-Hermann. Thanks also to the members of the PhD examination committee for kindly accepting the invitation and for taking their time.

Many thanks to my colleagues (students, postdocs, TAs and Frauke), who helped a lot with scientific advice, techniques, instruments, mice, reagents, organizational stuff… At least of equal importance were the many nice words in difficult moments, drinking coffee together, sharing chocolate and other sweets, watching movies, barbecuing and swimming in the Heidbergsee.

Danke, Stammtisch, dass ihr so geduldig seid und unsere Freundschaft nicht aufgegeben habt, obwohl ich so oft keine Zeit hatte, mit euch etwas zu unternehmen.

Danke Martin, Jutta und Marlene. Eure Unterstützung war essenziell. Ohne euch und ohne die Momente, die wir zusammen verbracht haben, wäre das deutlich langweiliger gewesen. Die Fahrradtouren, der Weihnachtsmarkt in Eppstein, die schönen Wochenende in Hannover und in Braunschweig bleiben unvergesslich.

Nicola, ganz besonders will ich mich bei dir bedanken. Danke für die Geduld, die du aufgebracht hast, z. B. wenn du in den Urlaub fahren wolltest und ich nicht konnte oder wenn ich am Wochenende arbeiten musste und es nicht mit dir verbringen konnte... Danke für die Unterstützung, ich werde alles versuchen, sie dir in den nächsten Schritten unseres Lebens zurückzugeben.

Mainha, painho, Lucas e André. Vocês são a razão da minha força pra acordar todo dia de manhã, ir pro trabalho e me dedicar ao máximo pra alcançar meus sonhos. Vocês me ensinaram a acreditar, ter disciplina, ter honestidade e tentar construir um mundo melhor. Foram exatamente esses ensinamentos que me trouxeram até aqui! Esse trabalho eu dedico a vocês.

Publications

Khailaie S., Bahrami F., Janahmadi M., Milanez-Almeida P., Huehn J., Meyer-Hermann M. **A mathematical model of immune activation with a unified self-nonself concept.** *Front Immunol*. 2013 Dec 26;4:474. doi: 10.3389/fimmu.2013.00474.

Herder V., Gerhauser I., Klein S.K., Almeida P., Kummerfeld M., Ulrich R., Seehusen F., Rohn K., Schaudien D., Baumgärtner W., Huehn J., Beineke A. **Interleukin-10 expression during the acute phase is a putative prerequisite for delayed viral elimination in a murine model for multiple sclerosis.** *J Neuroimmunol*. 2012 Aug 15;249(1-2):27-39. doi: 10.1016/j.jneuroim.2012.04.010.

In Revision

Milanez-Almeida P., Meyer-Hermann M., Toker A., Khailaie S., Huehn J. **Foxp3$^+$ regulatory T cell homeostasis quantitatively differs in murine peripheral lymph nodes and spleen.**

In Preparation

Milanez-Almeida P., Glage S., Schughart K., Schultze J.L., Lutz M.B., Huehn J. **Myeloid-derived suppressor cells in influenza A-infected mice.**

Milanez-Almeida P., Klawonn F., Huehn J. **Differential control of immune cell subsets by Foxp3$^+$ regulatory T cells in peripheral lymph nodes and spleen.**